Conventional and topological realizations of nanoscopic superconductivity

Tadeusz DOMAŃSKI

M. Curie-Skłodowska University (Lublin)

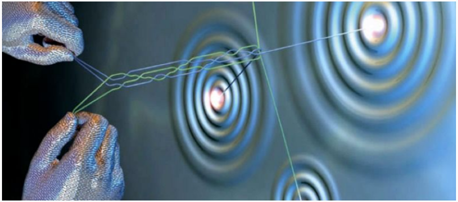

Zjazd Fizyków Polskich (Bydgoszcz) **20 IX 2021**

I. Superconductivity of nanoscopic samples:

OUTLINE

I. Superconductivity of nanoscopic samples:

$\Rightarrow$ **magnetism vs. pairing**

$\Rightarrow$ **topological phases**

$\Rightarrow$ **Majorana quasiparticles**

OUTLINE

I. Superconductivity of nanoscopic samples:

$\Rightarrow$ **magnetism vs. pairing**

$\Rightarrow$ **topological phases**

$\Rightarrow$ **Majorana quasiparticles**

II. Superconductivity in time-domain:

$\Rightarrow$ **dynamical phase transition**

Macroscopic superconductors

SUPERCONDUCTOR: PROPERTIES

Perfect conductor

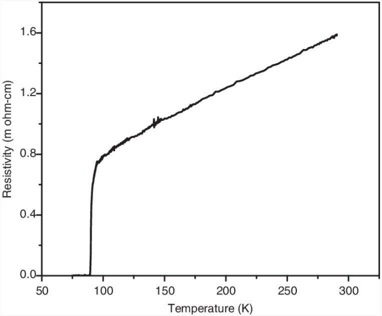

Perfect conductor

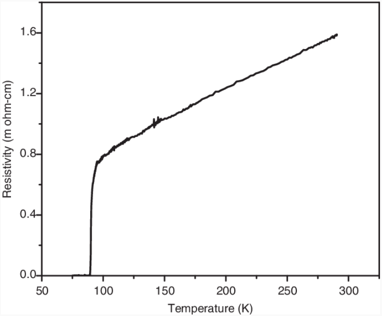

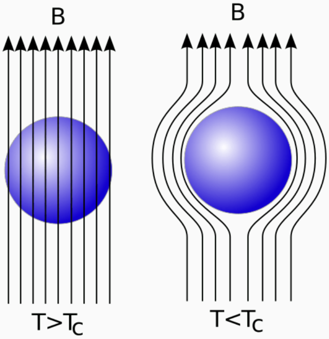

Perfect diamagnet

ELECTRON PAIRING

BCS (non-Fermi liquid) ground state :

$$|\mathbf{BCS}\rangle = \prod_k \left(u_k + v_k \, \hat{c}^\dagger_{k\uparrow} \, \hat{c}^\dagger_{-k\downarrow} \right) \; |\mathbf{vacuum}\rangle$$

ELECTRON PAIRING

BCS (non-Fermi liquid) ground state :

$$|\mathbf{BCS}\rangle = \prod_k \left(u_k + v_k \; \hat{c}^\dagger_{k\uparrow} \, \hat{c}^\dagger_{-k\downarrow} \right) \; |\mathbf{vacuum}\rangle$$

$|v_k|^2 \Rightarrow$ **probablity of occupied states** $(k\uparrow, -k\downarrow)$

ELECTRON PAIRING

BCS (non-Fermi liquid) ground state :

$$|\mathbf{BCS}\rangle = \prod_k \left(u_k + v_k \, \hat{c}^\dagger_{k\uparrow} \, \hat{c}^\dagger_{-k\downarrow} \right) \, |\mathbf{vacuum}\rangle$$

$|v_k|^2 \Rightarrow$ **probablity of occupied states** $(k \uparrow, -k \downarrow)$

$|u_k|^2 \Rightarrow$ **probablity of unoccupied states** $(k \uparrow, -k \downarrow)$

ELECTRON PAIRING

BCS (non-Fermi liquid) ground state :

$$|\mathrm{BCS}\rangle = \prod_k \left(u_k + v_k \, \hat{c}^\dagger_{k\uparrow} \, \hat{c}^\dagger_{-k\downarrow} \right) \; |\mathbf{vacuum}\rangle$$

$|v_k|^2 \Rightarrow$ **probablity of occupied states** $(k \uparrow, -k \downarrow)$

$|u_k|^2 \Rightarrow$ **probablity of unoccupied states** $(k \uparrow, -k \downarrow)$

Bogoliubov quasiparticle = superposition of a particle and hole

$$\begin{aligned} \hat{\gamma}_{k\uparrow} &= u_k \hat{c}_{k\uparrow} + v_k \hat{c}^\dagger_{-k\downarrow} \\ \hat{\gamma}^\dagger_{-k\downarrow} &= -v_k \hat{c}_{k\uparrow} + u_k \hat{c}^\dagger_{-k\downarrow} \end{aligned}$$

ELECTRON PAIRING

BCS (non-Fermi liquid) ground state :

$$|\mathrm{BCS}\rangle = \prod_k \left(u_k + v_k \; \hat{c}^\dagger_{k\uparrow} \; \hat{c}^\dagger_{-k\downarrow} \right) \; |\mathrm{vacuum}\rangle$$

$|v_k|^2 \Rightarrow$ **probablity of occupied states** $(k \uparrow, -k \downarrow)$

$|u_k|^2 \Rightarrow$ **probablity of unoccupied states** $(k \uparrow, -k \downarrow)$

Bogoliubov quasiparticle = superposition of a particle and hole

$$\begin{aligned} \hat{\gamma}_{k\uparrow} &= u_k \hat{c}_{k\uparrow} + v_k \hat{c}^\dagger_{-k\downarrow} \\ \hat{\gamma}^\dagger_{-k\downarrow} &= -v_k \hat{c}_{k\uparrow} + u_k \hat{c}^\dagger_{-k\downarrow} \end{aligned}$$

Charge is conserved modulo-2e due to Bose-Einstein condensation of Cooper pairs

$$\begin{aligned} \hat{\gamma}_{k\uparrow} &= u_k \hat{c}_{k\uparrow} + \tilde{v}_k \; \hat{b}_{q=0} \hat{c}^\dagger_{-k\downarrow} \\ \hat{\gamma}^\dagger_{-k\downarrow} &= -\tilde{v}_k \; \hat{b}^\dagger_{q=0} \; \hat{c}_{k\uparrow} + u_k \hat{c}^\dagger_{-k\downarrow} \end{aligned}$$

Quasiparticle spectrum of conventional superconductors consists of two Bogoliubov (p/h) branches, gaped around E_F

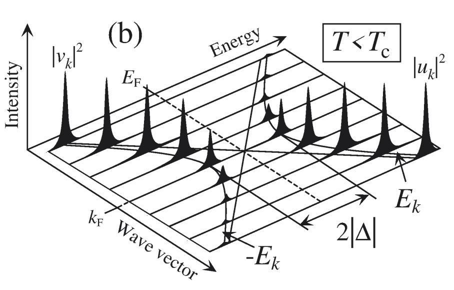

Quasiparticle spectrum of conventional superconductors consists of two Bogoliubov (p/h) branches, gaped around E_F

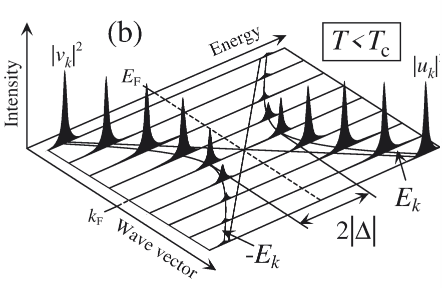

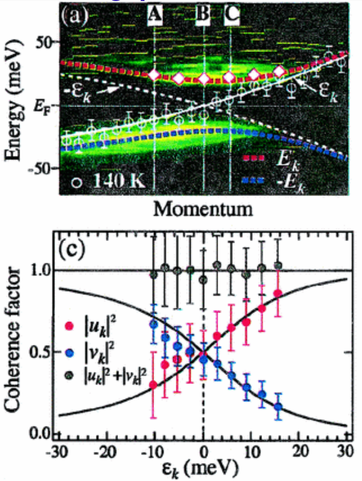

H. Matsui et al, Phys. Rev. Lett. 90, 217002 (2003).

PARTICLE VS HOLE

In all superconductors the particle and hole degrees of freedom are mixed with one another

PARTICLE VS HOLE

In all superconductors the particle and hole degrees of freedom are mixed with one another (this is particularly evident near E_F)

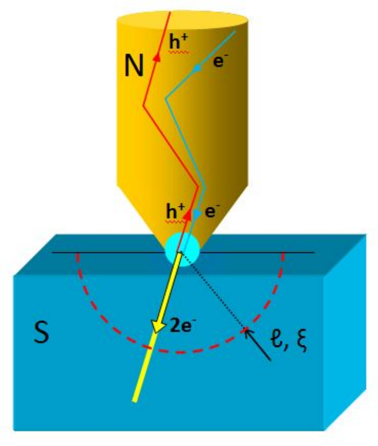

PARTICLE VS HOLE

Let us consider the interface of metal N and superconductor S

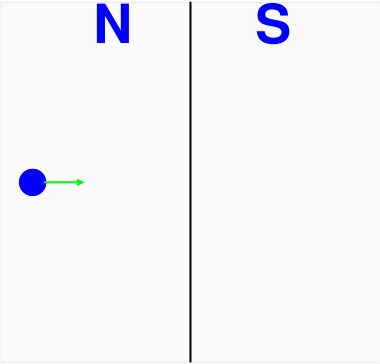

where incident electron ...

PARTICLE VS HOLE

Let us consider the interface of metal N and superconductor S

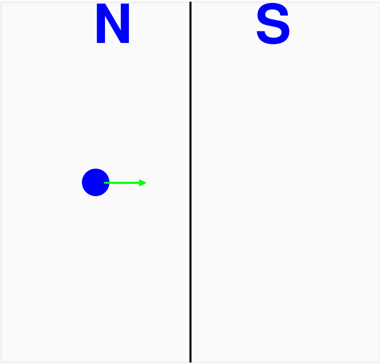

where incident electron ...

PARTICLE VS HOLE

Let us consider the interface of metal N and superconductor S

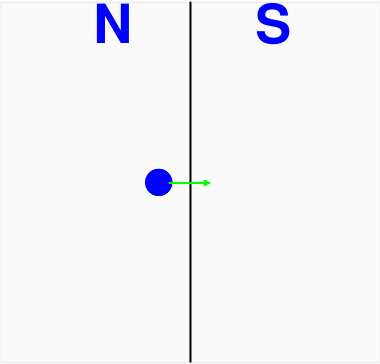

where incident electron ...

PARTICLE VS HOLE

Let us consider the interface of metal N and superconductor S

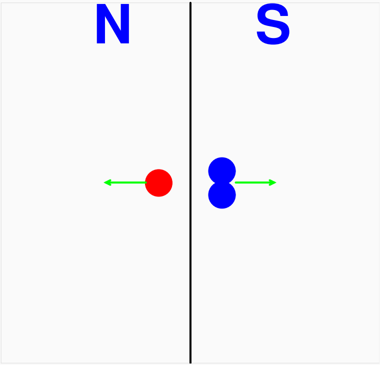

where incident electron is converted into: Cooper pair + hole.

Let us consider the interface of metal **N** and superconductor **S**

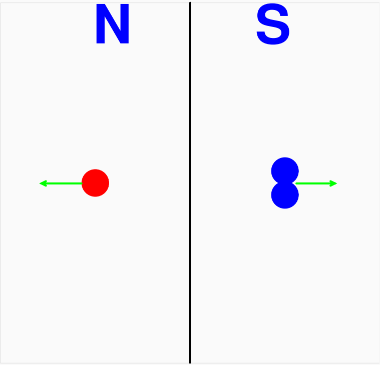

where incident electron is converted into: Cooper pair + hole.

PARTICLE VS HOLE

Let us consider the interface of metal N and superconductor S

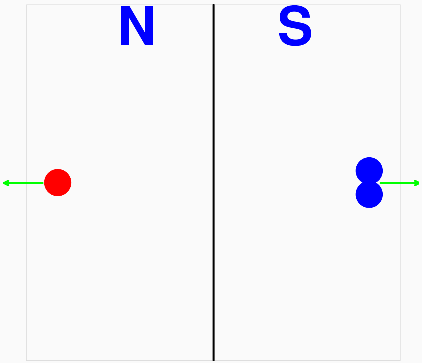

where incident electron is converted into: Cooper pair + hole.

Influence of magnetic field

Influence of magnetic field

Pairing vs magnetism: are they friends or foes ?

CRITICAL MAGNETIC FIELD

Magnetism and superconductivity seem to be rather antagonistic ...

CRITICAL MAGNETIC FIELD

Magnetism and superconductivity seem to be rather antagonistic ...

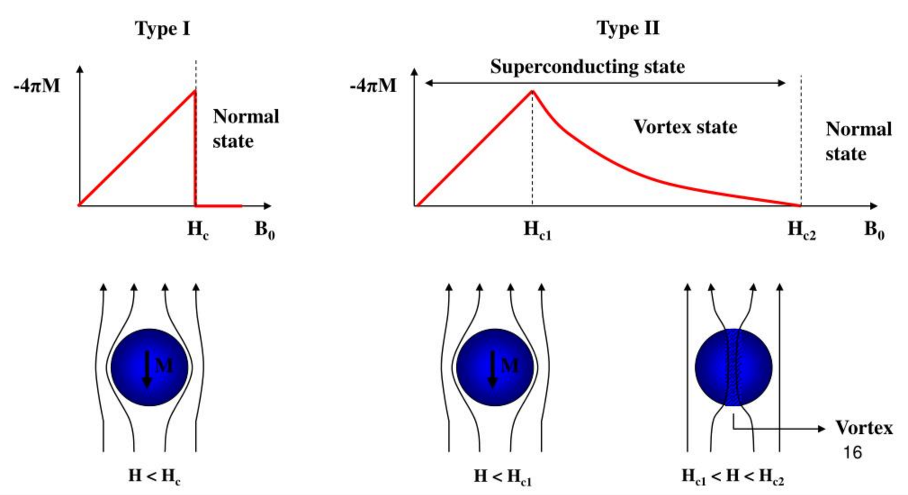

In type-II superconductors the magnetic field can partly penetrate a sample

MIXED STATE

Partial leakage of the magnetic field into the sample takes a form of the quantized vortices, arranged in the Abrikosov lattice.

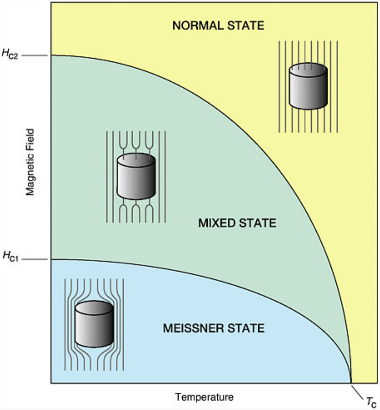

MIXED STATE

Partial leakage of the magnetic field into the sample takes a form of the quantized vortices, arranged in the Abrikosov lattice.

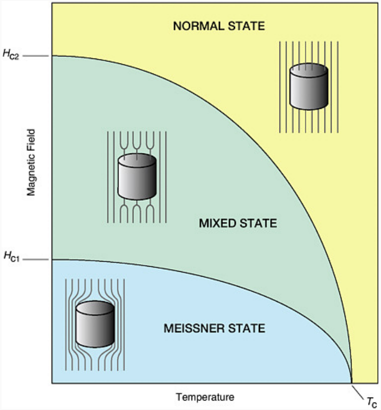

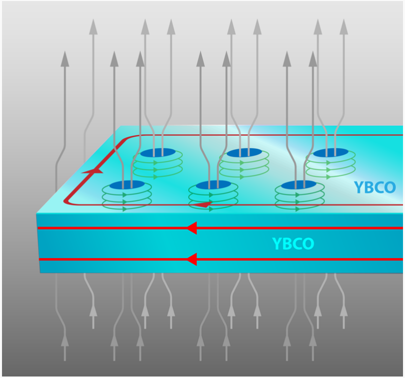

VORTEX IN SUPERCONDUCTOR

A single vortex encloses the magnetic field flux $\Phi = \frac{h}{2e}$.

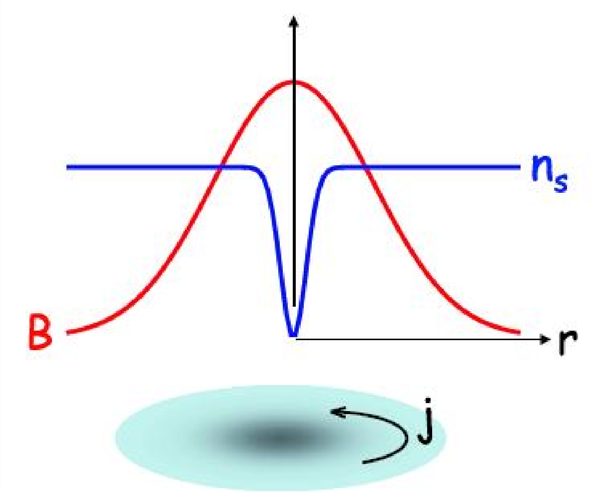

Vortex can be regarded as a piece of *normal* region in superconductor.

PROBING BOUND STATES CONFINED VORTEX

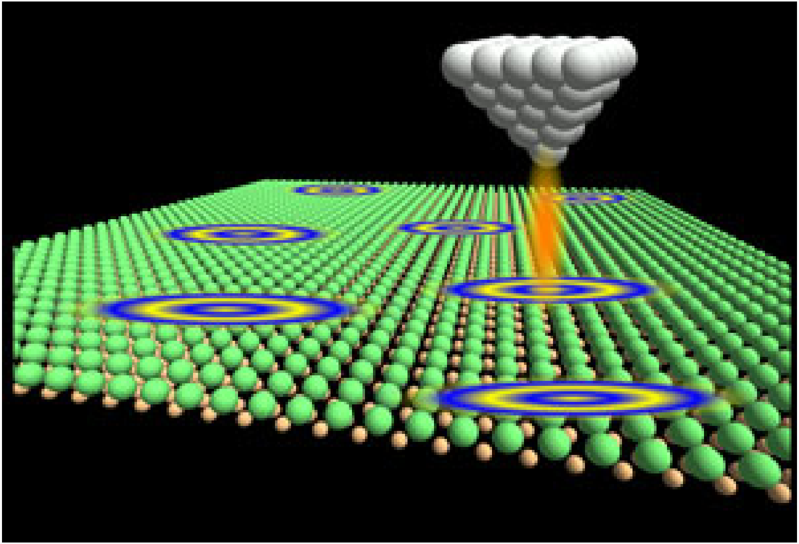

Natural method for probing the local (bound) states could be STM.

STATES BOUND TO VORTEX CORE

Volume 9, number 4 PHYSICS LETTERS 1 May 1964

BOUND FERMION STATES ON A VORTEX LINE IN A TYPE II SUPERCONDUCTOR

C. CAROLI, P. G. DE GENNES, J. MATRICON
Service de Physique des Solides, Faculté des Sciences, Orsay (S & O)

Vortex can be regarded as a scattering center for propagating quasiparticles.

STATES BOUND TO VORTEX CORE

Volume 9, number 4 PHYSICS LETTERS 1 May 1964

BOUND FERMION STATES ON A VORTEX LINE IN A TYPE II SUPERCONDUCTOR

C. CAROLI, P. G. DE GENNES, J. MATRICON
Service de Physique des Solides, Faculté des Sciences, Orsay (S & O)

Vortex can be regarded as a scattering center for propagating quasiparticles. The resulting bound-states of axisymmetric vortex in s-wave superconductors take a form:

$$E_n = \omega_0 \left(n + \frac{1}{2} \right) \qquad n = 0, \pm 1, \pm 2, \ldots$$

STATES BOUND TO VORTEX CORE

Volume 9, number 4 PHYSICS LETTERS 1 May 1964

BOUND FERMION STATES ON A VORTEX LINE IN A TYPE II SUPERCONDUCTOR

C. CAROLI, P. G. DE GENNES, J. MATRICON
Service de Physique des Solides, Faculté des Sciences, Orsay (S & O)

Vortex can be regarded as a scattering center for propagating quasiparticles. The resulting bound-states of axisymmetric vortex in s-wave superconductors take a form:

$$E_n = \omega_0 \left(n + \frac{1}{2} \right) \qquad\qquad n = 0, \pm 1, \pm 2, \ldots$$

where

$$\omega_0 \approx \frac{\Delta^2}{E_F}$$

RESOLVING DISCRETE LEVELS OF VORTEX

STM evidence for Caroli - de Gennes - Matricon states in $FeTe_{0.55}Se_{0.45}$

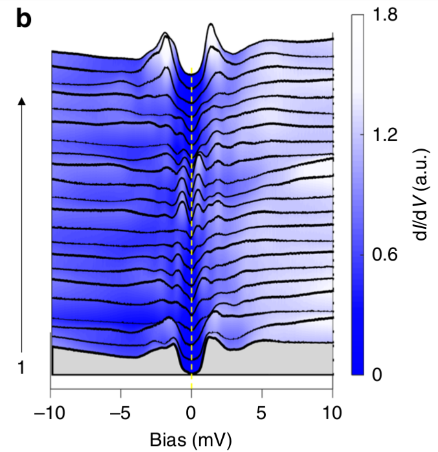

RESOLVING DISCRETE LEVELS OF VORTEX

STM evidence for Caroli - de Gennes - Matricon states in $FeTe_{0.55}Se_{0.45}$

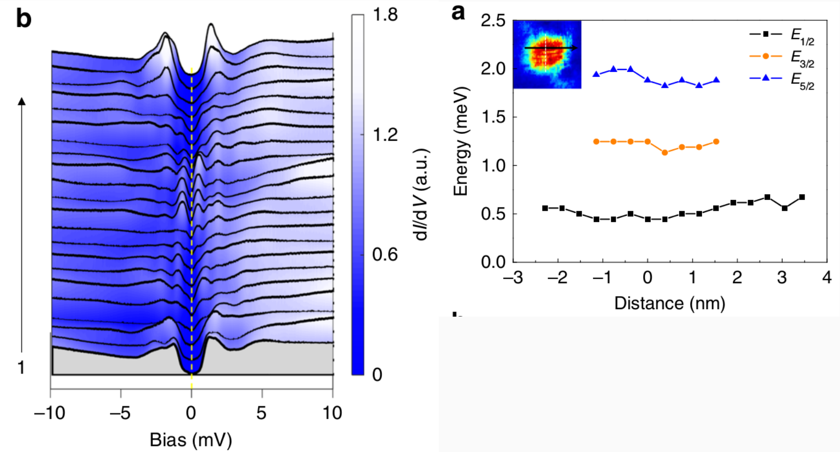

STM evidence for Caroli - de Gennes - Matricon states in $FeTe_{0.55}Se_{0.45}$

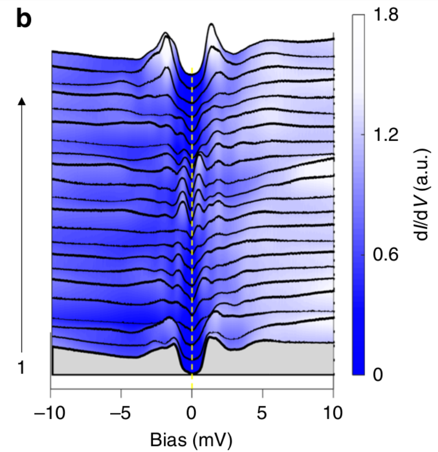

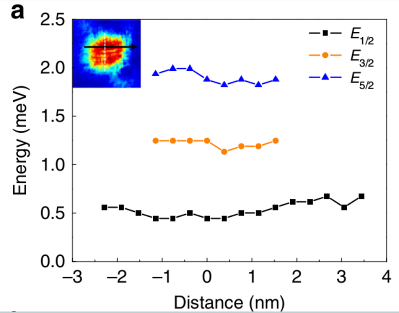

nature COMMUNICATIONS

ARTICLE

DOI: 10.1038/s41467-018-03404-8 OPEN

Discrete energy levels of Caroli-de Gennes-Matricon states in quantum limit in $FeTe_{0.55}Se_{0.45}$

Mingyang Chen[1], Xiaoyu Chen[1], Huan Yang[1], Zengyi Du[1], Xiyu Zhu[1], Enyu Wang[1] & Hai-Hu Wen[1]

Data for $T = 0.4$ K ($T_c = 13.3$ K)

M. Chen et al., Nature Comm. 9, 970 (2018).

VORTEX IN P-WAVE SUPERCONDUCTOR

JETP LETTERS VOLUME 70, NUMBER 9 10 NOV. 1999

Fermion zero modes on vortices in chiral superconductors

G. E. Volovik

Helsinki University of Technology, Low Temperature Laboratory, FIN-02015 HUT, Finland; Landau Institute of Theoretical Physics, Russian Academy of Sciences, 117334 Moscow, Russia

(Submitted 30 September 1999)
Pis'ma Zh. Éksp. Teor. Fiz. **70**, No. 9, 601–606 (10 November 1999)

Bound-states of the vortex in p-wave (triplet) superconductors are given by:

$$E_n = \omega_0 n \qquad\qquad n = 0, \pm 1, \pm 2, \ldots$$

VORTEX IN P-WAVE SUPERCONDUCTOR

JETP LETTERS VOLUME 70, NUMBER 9 10 NOV. 1999

Fermion zero modes on vortices in chiral superconductors

G. E. Volovik

Helsinki University of Technology, Low Temperature Laboratory, FIN-02015 HUT, Finland; Landau Institute of Theoretical Physics, Russian Academy of Sciences, 117334 Moscow, Russia

(Submitted 30 September 1999)
Pis'ma Zh. Éksp. Teor. Fiz. **70**, No. 9, 601–606 (10 November 1999)

Bound-states of the vortex in p-wave (triplet) superconductors are given by:

$$E_n = \omega_0 n \qquad\qquad n = 0, \pm 1, \pm 2, \ldots$$

implying the bound state at zero-energy !

BOUND STATES IN A VORTEX (EXPERIMENT)

$FeTe_{0.55}Se_{0.45}$ superconductor ($T_c = 14.5$ K, $\Delta = 1.8$ meV, $E_F = 4.4$ meV).

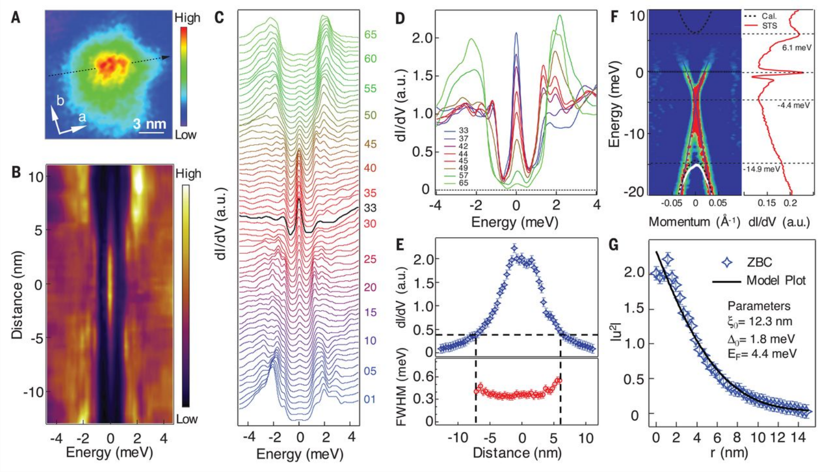

D. Wang et al, Science 362, 333 (2018) /Chinese Academy of Sciences (Beijing)/

BOUND STATES IN A VORTEX (EXPERIMENT)

"It is technically possible to move a vortex by STM tip, which in principle can be used to exchange the Majorana bound states inside vortices."

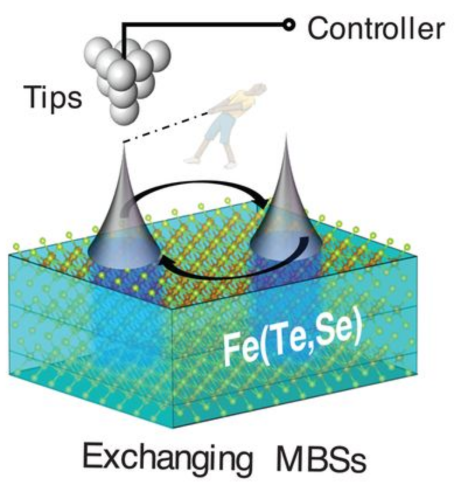

BOUND STATES IN A VORTEX (EXPERIMENT)

"It is technically possible to move a vortex by STM tip, which in principle can be used to exchange the Majorana bound states inside vortices."

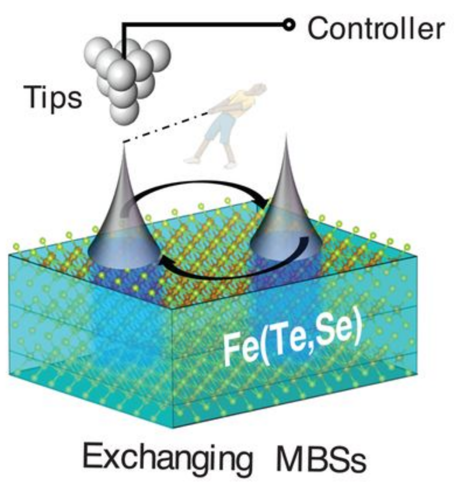

zero-energy state = Majorana ? $\Leftarrow$ highly controversial claim

Nanoscale superconductors

IMPURITY IN BULK SUPERCONDUCTOR

Typical spectrum of a single impurity in s-wave superconductor:

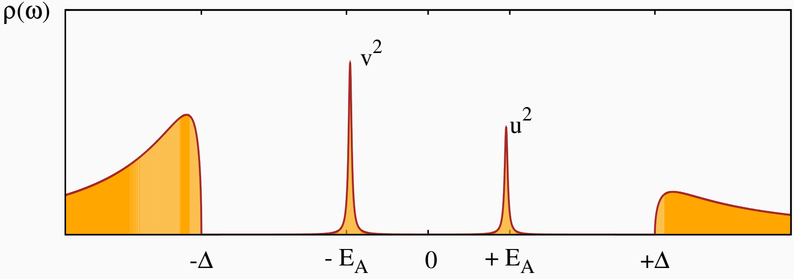

Bound states appearing in the subgap region $E \in \langle -\Delta, \Delta \rangle$

Typical spectrum of a single impurity in s-wave superconductor:

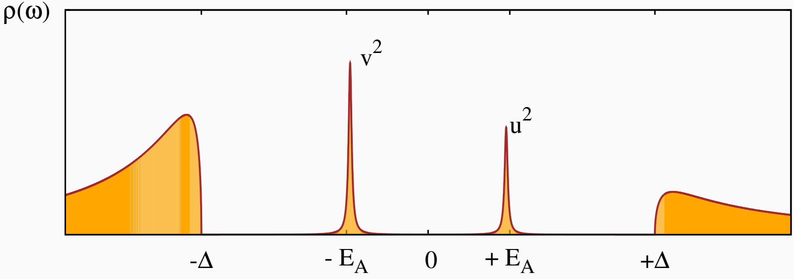

Bound states appearing in the subgap region $E \in \langle -\mathbf{\Delta}, \mathbf{\Delta} \rangle$

are dubbed Yu-Shiba-Rusinov (or Andreev) quasiparticles.

Other entities in superconductors, like magnetic chains

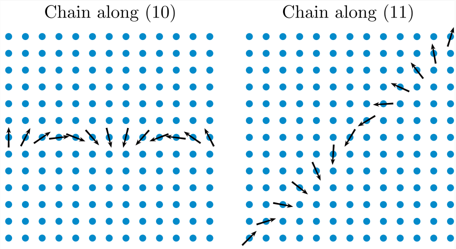

MAGNETIC OBJECTS IN SUPERCONDUCTORS

Other entities in superconductors, like magnetic chains

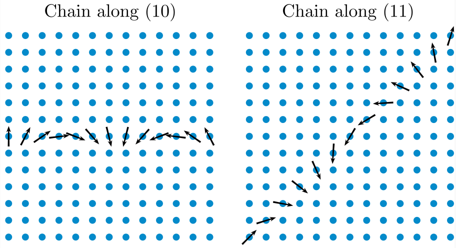

or magnetic islands

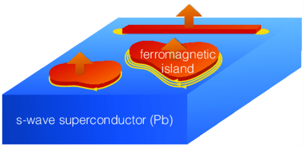

MAGNETIC OBJECTS IN SUPERCONDUCTORS

Other entities in superconductors, like magnetic chains

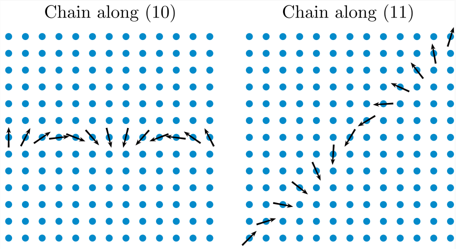

or magnetic islands

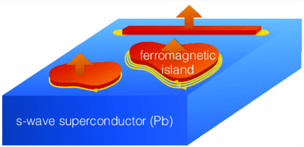

develop their in-gap bound states in a form of the Shiba-bands.

MAGNETIC OBJECTS IN SUPERCONDUCTORS

Other entities in superconductors, like magnetic chains

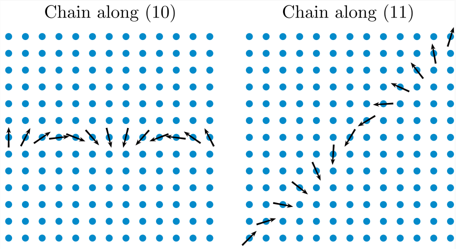

or magnetic islands

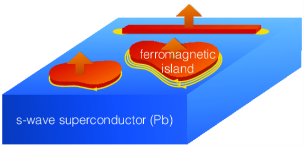

develop their in-gap bound states in a form of the Shiba-bands.

In particular, the proper magnetic textures in chains and islands can guarantee their topologically non-trivial character, hosting the exotic Majorana-type boundary modes !

Comment on topology (in physics)

The electric flux emanating from or flowing into a closed surface depends only on the total charge enclosed inside it. Particular details of such surface and the spatial charge distribution are irrelevant.

$$\oint \vec{E} \cdot \vec{dA} = \frac{Q}{\varepsilon_0}$$

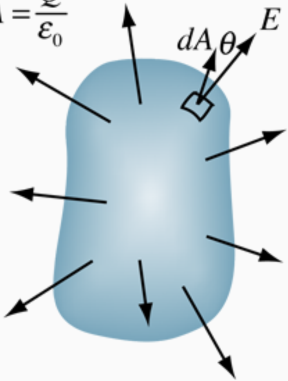

Johann Carl Friedrich Gauss (1777-1855)

TOPOLOGY OF ELECTRONIC STATES

In condensed matter physics we are concerned with the Bloch waves

$$\psi_{n,\vec{k}}(\vec{r}) = u_{n,\vec{k}}(\vec{r})\ e^{i\vec{k}\cdot\vec{r}}$$

with periodic $u_{n,\vec{k}}(\vec{r}+\vec{R}) = u_{n,\vec{k}}(\vec{r})$**.**

In condensed matter physics we are concerned with the Bloch waves

$$\psi_{n,\vec{k}}(\vec{r}) = u_{n,\vec{k}}(\vec{r})\; e^{i\vec{k}\cdot\vec{r}}$$

with periodic $u_{n,\vec{k}}(\vec{r}+\vec{R}) = u_{n,\vec{k}}(\vec{r})$**. The Schrödinger equation**

$$\hat{H}\;\psi_{n,\vec{k}}(\vec{r}) = \varepsilon_n(\vec{k})\psi_{n,\vec{k}}(\vec{r})$$

TOPOLOGY OF ELECTRONIC STATES

In condensed matter physics we are concerned with the Bloch waves

$$\psi_{n,\vec{k}}(\vec{r}) = u_{n,\vec{k}}(\vec{r})\ e^{i\vec{k}\cdot\vec{r}}$$

with periodic $u_{n,\vec{k}}(\vec{r}+\vec{R}) = u_{n,\vec{k}}(\vec{r})$. The Schrödinger equation

$$\hat{H}\ \psi_{n,\vec{k}}(\vec{r}) = \varepsilon_n(\vec{k})\psi_{n,\vec{k}}(\vec{r})$$

implies the gapped electronic spectra $\varepsilon_n(\vec{k})$ of bulk materials.

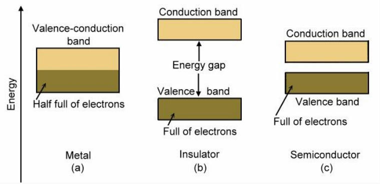

TOPOLOGY OF ELECTRONIC STATES

In condensed matter physics we are concerned with the Bloch waves

$$\psi_{n,\vec{k}}(\vec{r}) = u_{n,\vec{k}}(\vec{r})\ e^{i\vec{k}\cdot\vec{r}}$$

with periodic $u_{n,\vec{k}}(\vec{r}+\vec{R}) = u_{n,\vec{k}}(\vec{r})$. The Schrödinger equation

$$\hat{H}\ \psi_{n,\vec{k}}(\vec{r}) = \varepsilon_n(\vec{k})\psi_{n,\vec{k}}(\vec{r})$$

implies the gapped electronic spectra $\varepsilon_n(\vec{k})$ of bulk materials.

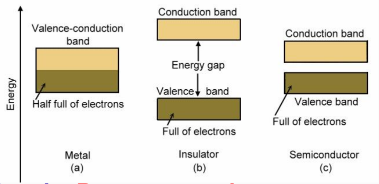

Additionally inspecting the Berry connection

$$\vec{A}_n(\vec{k}) = \left\langle u_{n,\vec{k}}(\vec{r}) \middle| i\nabla_{\vec{k}} \middle| u_{n,\vec{k}}(\vec{r}) \right\rangle$$

TOPOLOGY OF ELECTRONIC STATES

In condensed matter physics we are concerned with the Bloch waves

$$\psi_{n,\vec{k}}(\vec{r}) = u_{n,\vec{k}}(\vec{r})\ e^{i\vec{k}\cdot\vec{r}}$$

with periodic $u_{n,\vec{k}}(\vec{r}+\vec{R}) = u_{n,\vec{k}}(\vec{r})$. The Schrödinger equation

$$\hat{H}\ \psi_{n,\vec{k}}(\vec{r}) = \varepsilon_n(\vec{k})\psi_{n,\vec{k}}(\vec{r})$$

implies the gapped electronic spectra $\varepsilon_n(\vec{k})$ of bulk materials.

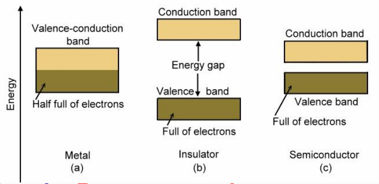

Additionally inspecting the Berry connection

$$\vec{A}_n(\vec{k}) = \left\langle u_{n,\vec{k}}(\vec{r}) \middle| i\nabla_{\vec{k}} \middle| u_{n,\vec{k}}(\vec{r}) \right\rangle$$

we can discover important details due to topology.

CONCEPTS OF BERRY-OLOGY

Using a gauge-invariant form of the Berry connection

$$\vec{A}_n(\vec{k}) \rightarrow \vec{A}_n(\vec{k}) - \nabla_{\vec{k}}\phi_n(\vec{k})$$

CONCEPTS OF BERRY-OLOGY

Using a gauge-invariant form of the Berry connection

$$\vec{A}_n(\vec{k}) \to \vec{A}_n(\vec{k}) - \nabla_{\vec{k}}\phi_n(\vec{k})$$

one can define the Berry curvature

$$\vec{F}_n(\vec{k}) = \nabla_{\vec{k}} \times \vec{A}_n(\vec{k})$$

Using a gauge-invariant form of the Berry connection

$$\vec{A}_n(\vec{k}) \rightarrow \vec{A}_n(\vec{k}) - \nabla_{\vec{k}}\phi_n(\vec{k})$$

one can define the Berry curvature

$$\vec{F}_n(\vec{k}) = \nabla_{\vec{k}} \times \vec{A}_n(\vec{k})$$

whose integral along a closed path

$$\oint_C d\vec{k} \cdot \vec{F}_n(\vec{k})$$

Using a gauge-invariant form of the Berry connection

$$\vec{A}_n(\vec{k}) \to \vec{A}_n(\vec{k}) - \nabla_{\vec{k}}\phi_n(\vec{k})$$

one can define the Berry curvature

$$\vec{F}_n(\vec{k}) = \nabla_{\vec{k}} \times \vec{A}_n(\vec{k})$$

whose integral along a closed path

$$\oint_C d\vec{k} \cdot \vec{F}_n(\vec{k})$$

yields the Berry phase (sometimes identical with the Chern number).

When certain symmetries are imposed and a suitable path C is considered, the Berry phase is quantized and can be regarded as topological invariant which plays equivalent role to electric charge in the classical Gauss law.

TOPOLOGICAL PROPERTIES

★ **According to: a) time-reversal, b) particle-hole and c) chiral symmetries all materials can be classified into 10 different categories (ten-fold method).**

TOPOLOGICAL PROPERTIES

★ **According to: a) time-reversal, b) particle-hole and c) chiral symmetries all materials can be classified into 10 different categories (ten-fold method).**

★ **Two materials belong to the same topological category, if there exists an adiabatic (continuous) process connecting them (preserving the gap).**

TOPOLOGICAL PROPERTIES

★ **According to: a) time-reversal, b) particle-hole and c) chiral symmetries all materials can be classified into 10 different categories (ten-fold method).**

★ **Two materials belong to the same topological category, if there exists an adiabatic (continuous) process connecting them (preserving the gap).**

★ **Topological transition occurs upon closing/reopening the gap,**

TOPOLOGICAL PROPERTIES

★ **According to: a) time-reversal, b) particle-hole and c) chiral symmetries all materials can be classified into 10 different categories (ten-fold method).**

★ **Two materials belong to the same topological category, if there exists an adiabatic (continuous) process connecting them (preserving the gap).**

★ **Topological transition occurs upon closing/reopening the gap, e.g.**

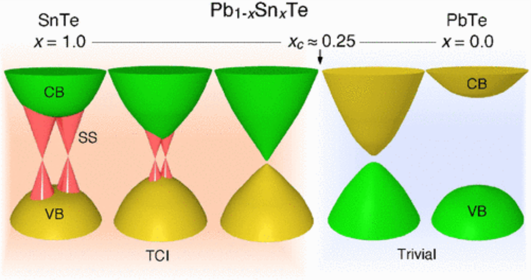

TOPOLOGICAL PROPERTIES

★ **According to: a) time-reversal, b) particle-hole and c) chiral symmetries all materials can be classified into 10 different categories (ten-fold method).**

★ **Two materials belong to the same topological category, if there exists an adiabatic (continuous) process connecting them (preserving the gap).**

★ **Topological transition occurs upon closing/reopening the gap, e.g.**

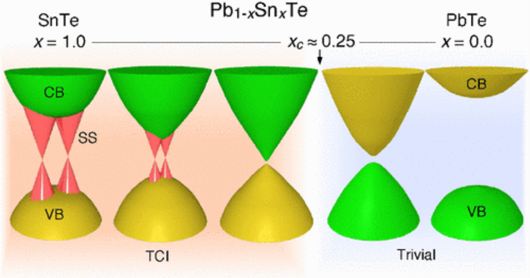

★ **Bulk-to-boundary correspondence assigns $2|\nu|$ edge modes related to the Chern number ν. These modes are topologically protected.**

$\Rightarrow$ **gaped structure of bulk superconductors is due to pairing**

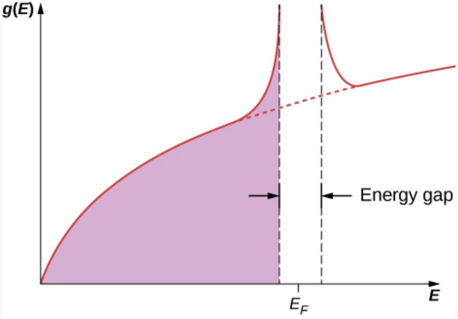

PROTOCOL FOR TOPOLOGICAL SUPERCONDUCTORS

⇒ **gaped structure of bulk superconductors is due to pairing**

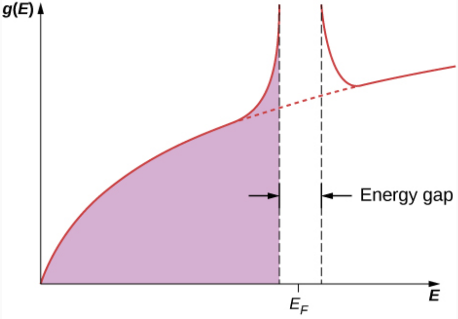

⇒ **clusters of magnetic impurities would in-gap Shiba bands**

PROTOCOL FOR TOPOLOGICAL SUPERCONDUCTORS

$\Rightarrow$ **gaped structure of bulk superconductors is due to pairing**

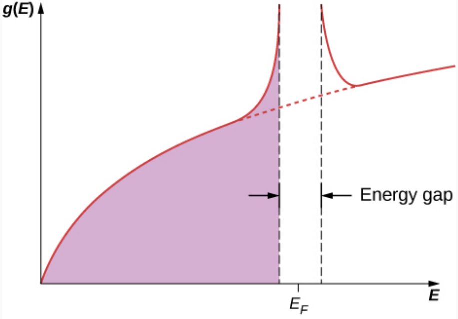

$\Rightarrow$ **clusters of magnetic impurities would in-gap Shiba bands**

$\Rightarrow$ **appropriate magnetic order can invert these Shiba bands**

PROTOCOL FOR TOPOLOGICAL SUPERCONDUCTORS

⇒ **gaped structure of bulk superconductors is due to pairing**

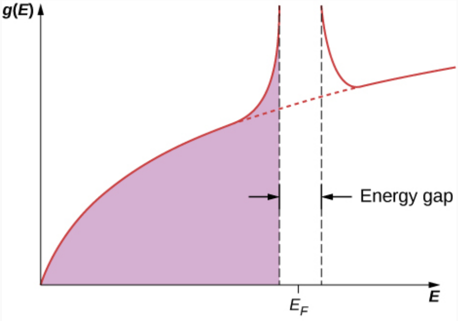

⇒ **clusters of magnetic impurities would in-gap Shiba bands**

⇒ **appropriate magnetic order can invert these Shiba bands**

In realistic situations more sophisticated reasoning is necessary !

A few examples ...

1. Rashba nanowires

TOPOLOGICAL SUPERCONDUCTING NANOWIRE

Pairing of identical spin electrons is driven by the spin-orbit (Rashba) interaction in presence of magnetic field, using the semiconducting nanowires proximitized to conventional (*s-wave*) superconductor.

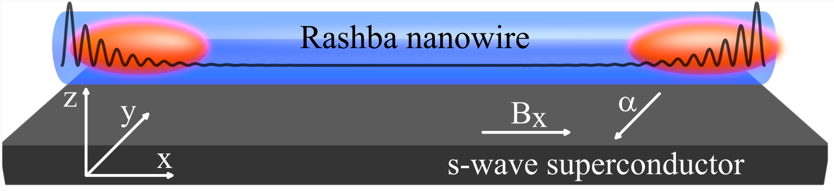

Effective quasiparticle states of the Rashba nanowire

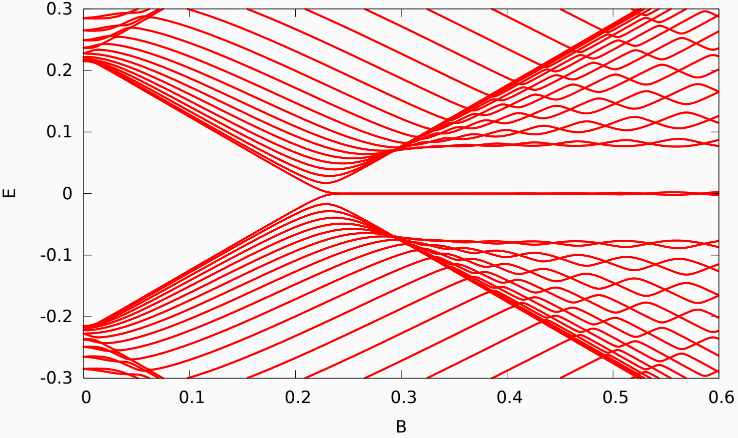

Effective quasiparticle states of the Rashba nanowire

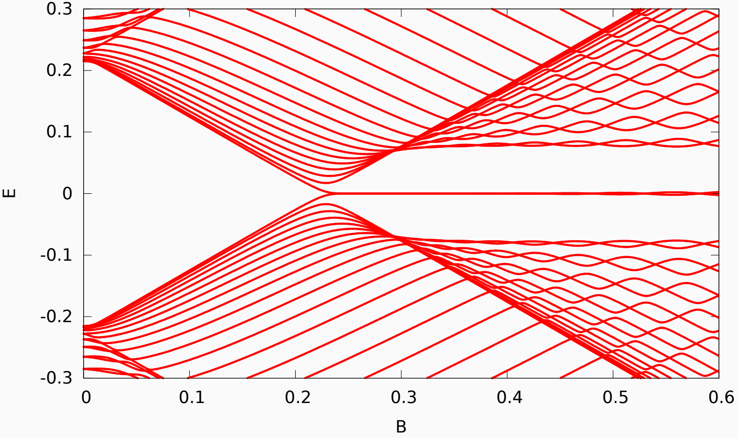

closing/reopening of a gap ⇔ band-invertion of topological insulators

M.M. Maśka, A. Gorczyca-Goraj, J. Tworzydło, T. Domański, PRB 95, 045429 (2017).

Majorana qps are localized near the edges

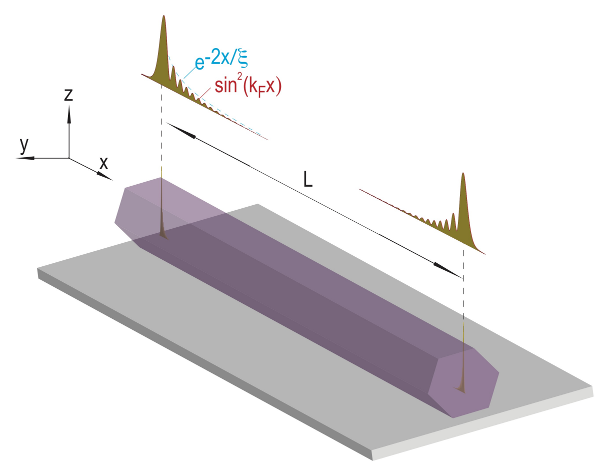

R. Aguado, Riv. Nuovo Cim. 40, 523 (2017).

EXAMPLE OF EMPIRICAL REALIZATION

Differential conductance dI/dV obtained for InSb nanowire at 70 mK upon varying a magnetic field.

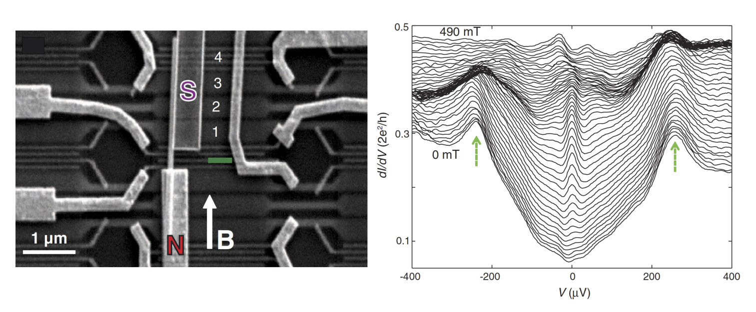

V. Mourik, ..., and L.P. Kouwenhoven, Science **336**, 1003 (2012).

/ Technical Univ. Delft, Netherlands /

Litographically fabricated Al nanowire contacted to InAs

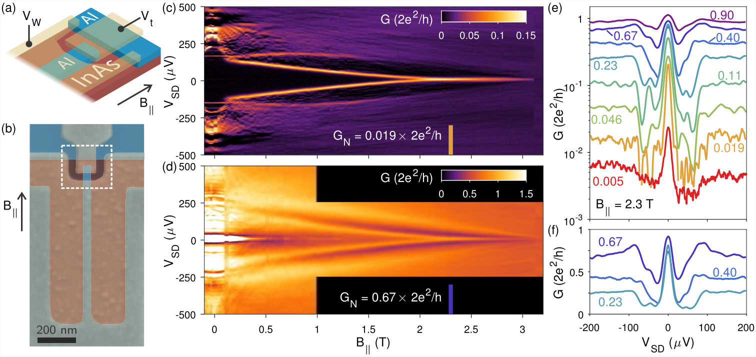

F. Nichele, ..., and Ch. Marcus, Phys. Rev. Lett. **119**, 136803 (2017).

/ Niels Bohr Institute, Copenhagen, Denmark /

Low energy quasiparticles of the Rashba nanowire

$t_{35}/t = 1.0$

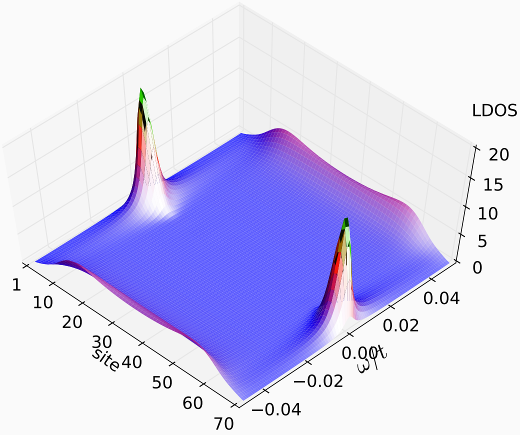

M.M. Maśka, A. Gorczyca-Goraj, J. Tworzydło, T. Domański, PRB 95, 045429 (2017).

Low energy quasiparticles of the Rashba nanowire

$t_{35}/t = 0.8$

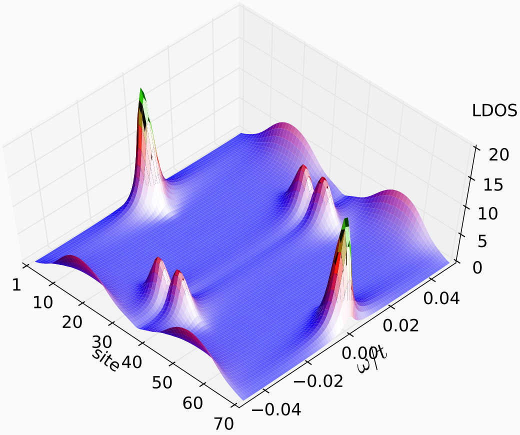

M.M. Maśka, A. Gorczyca-Goraj, J. Tworzydło, T. Domański, PRB 95, 045429 (2017).

Low energy quasiparticles of the Rashba nanowire

$t_{35}/t = 0.6$

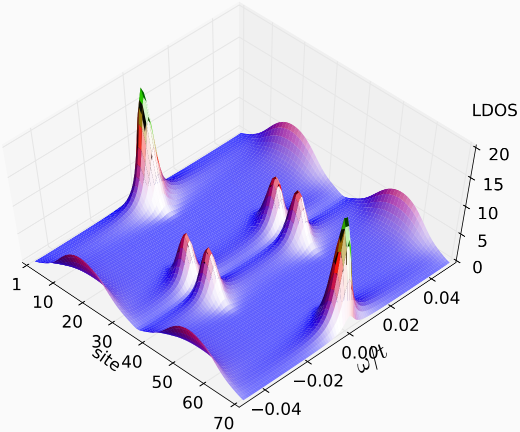

M.M. Maśka, A. Gorczyca-Goraj, J. Tworzydło, T. Domański, PRB 95, 045429 (2017).

Low energy quasiparticles of the Rashba nanowire

$t_{35}/t = 0.4$

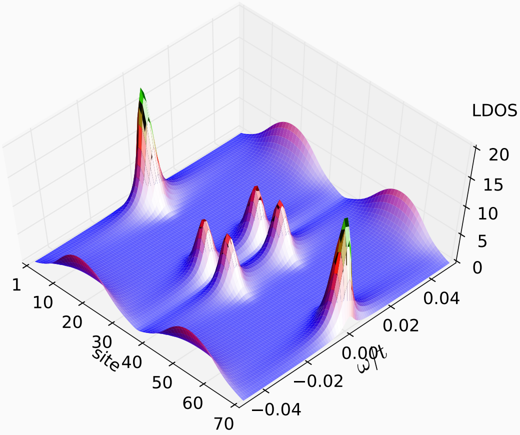

M.M. Maśka, A. Gorczyca-Goraj, J. Tworzydło, T. Domański, PRB 95, 045429 (2017).

Low energy quasiparticles of the Rashba nanowire

$t_{35}/t = 0.2$

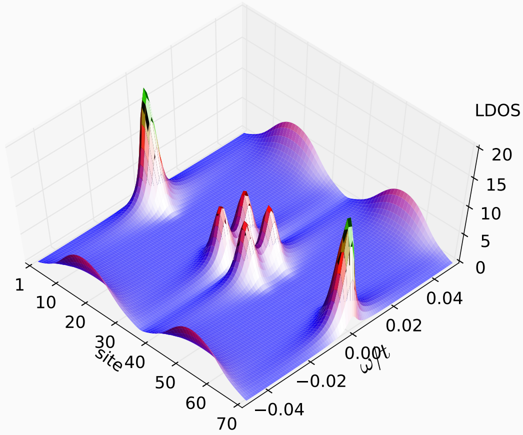

M.M. Maśka, A. Gorczyca-Goraj, J. Tworzydło, T. Domański, PRB 95, 045429 (2017).

Low energy quasiparticles of the Rashba nanowire

$t_{35}/t = 0.1$

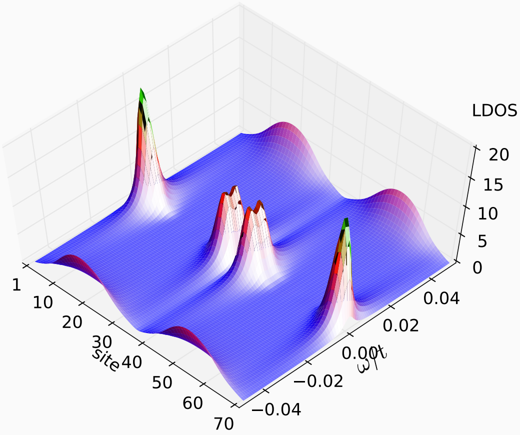

M.M. Maśka, A. Gorczyca-Goraj, J. Tworzydło, T. Domański, PRB 95, 045429 (2017).

Low energy quasiparticles of the Rashba nanowire

$t_{35}/t = 0.0$

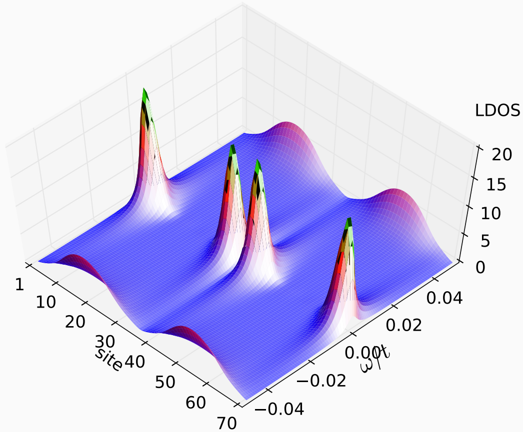

M.M. Maśka, A. Gorczyca-Goraj, J. Tworzydło, T. Domański, PRB 95, 045429 (2017).

2. Selforganised magnetic chains

MAGNETIC CHAINS ON SUPERCONDUCTORS

Magnetic atoms (like Fe) on a surface of s-wave superconductor (for example Pb) arrange themselves into such spiral order, where topological superconducting phase is selfsustained

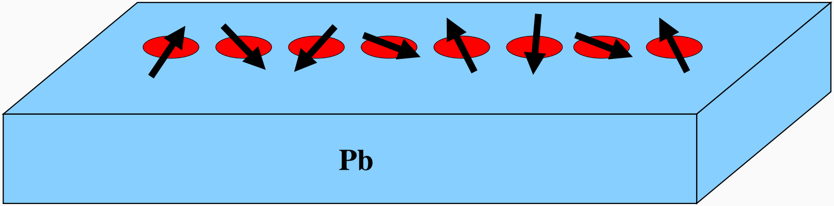

MICROSCOPIC MODEL

Itinerant electrons in the chain of magnetic impurities placed on a surface of isotropic superconductor can be described by the Hamiltonian:

$$
\begin{aligned}
H = & - t \sum_{i,\sigma} \left(\hat{c}^{\dagger}_{i,\sigma} \hat{c}_{i+1,\sigma} + \mathrm{H.c.} \right) - \mu \sum_{i,\sigma} \hat{c}^{\dagger}_{i,\sigma} \hat{c}_{i,\sigma} \\
& + J \sum_{i} \vec{S}_i \cdot \hat{\vec{s}}_i + \sum_{i} \left(\Delta \hat{c}^{\dagger}_{i\uparrow} \hat{c}^{\dagger}_{i\downarrow} + \mathrm{H.c.} \right)
\end{aligned}
$$

Here $\vec{S}_i$ are the classical magnetic moments and $\hat{\vec{s}}_i = \frac{1}{2} \sum_{\alpha,\beta} \hat{c}^{\dagger}_{i,\alpha} \vec{\sigma}_{\alpha\beta} \hat{c}_{i,\beta}$ denote the spins of mobile electrons

$\Longrightarrow$ J is the coupling between magnetic atoms and itinerant electrons

$\Longrightarrow$ Δ is the proximity induced on-site pairing

HELICAL SELFORGANISATION (TOPOFILIA)

A. Gorczyca-Goraj, T. Domański & M.M. Maśka, Phys. Rev. B 99, 235430 (2019).

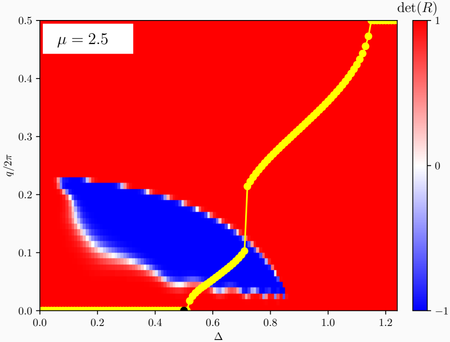

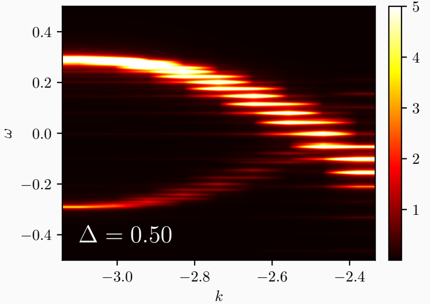

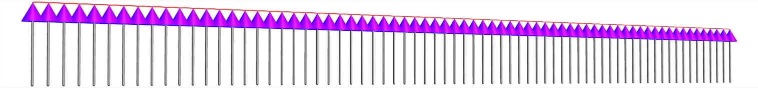

HELICAL SELFORGANISATION (TOPOFILIA)

A. Gorczyca-Goraj, T. Domański & M.M. Maśka, Phys. Rev. B 99, 235430 (2019).

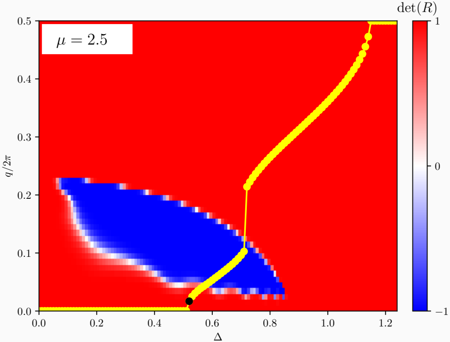

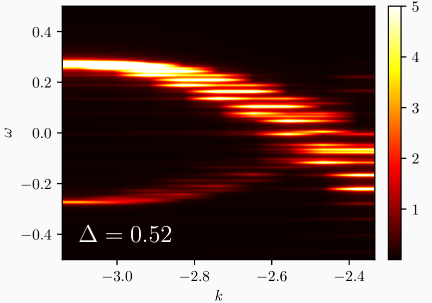

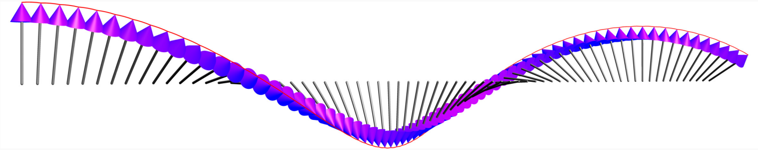

HELICAL SELFORGANISATION (TOPOFILIA)

A. Gorczyca-Goraj, T. Domański & M.M. Maśka, Phys. Rev. B 99, 235430 (2019).

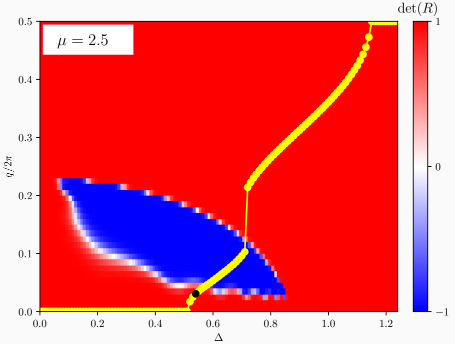

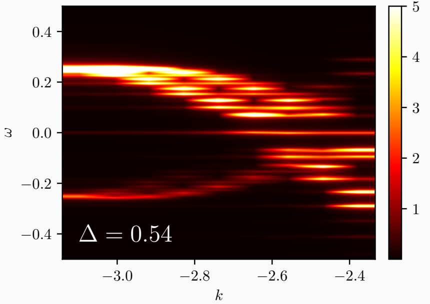

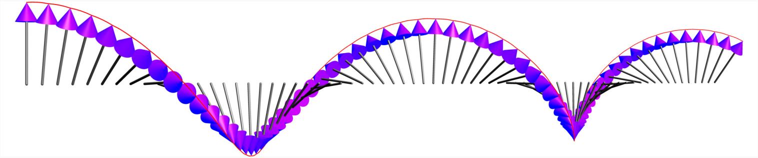

HELICAL SELFORGANISATION (TOPOFILIA)

A. Gorczyca-Goraj, T. Domański & M.M. Maśka, Phys. Rev. B 99, 235430 (2019).

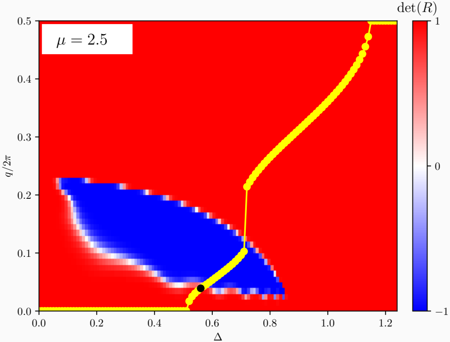

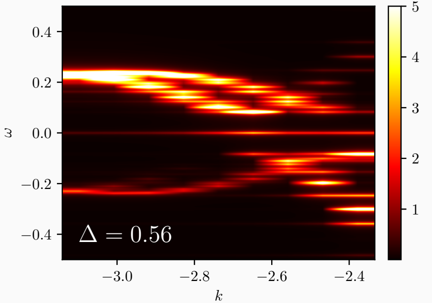

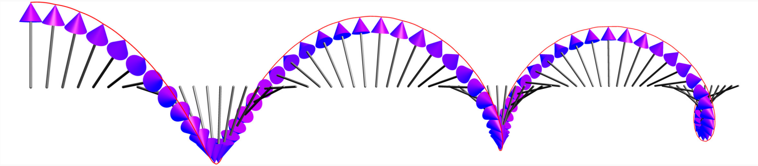

HELICAL SELFORGANISATION (TOPOFILIA)

A. Gorczyca-Goraj, T. Domański & M.M. Maśka, Phys. Rev. B 99, 235430 (2019).

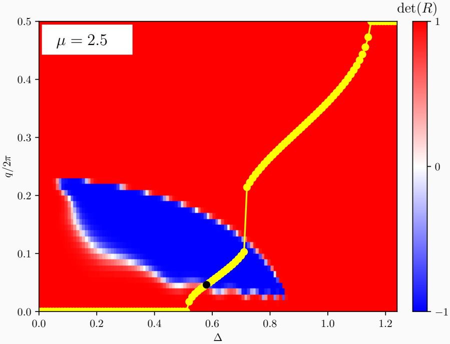

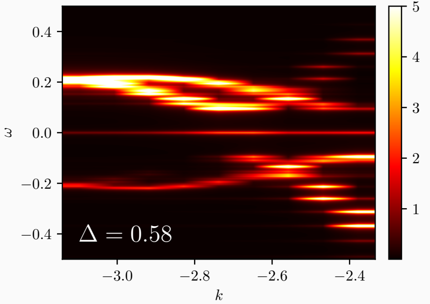

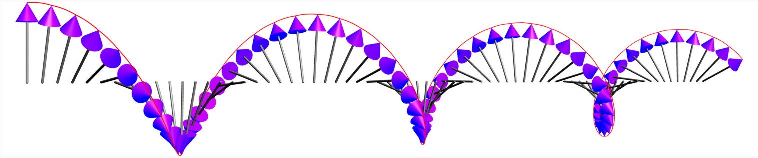

HELICAL SELFORGANISATION (TOPOFILIA)

A. Gorczyca-Goraj, T. Domański & M.M. Maśka, Phys. Rev. B 99, 235430 (2019).

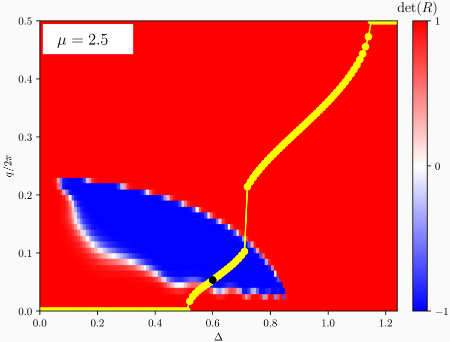

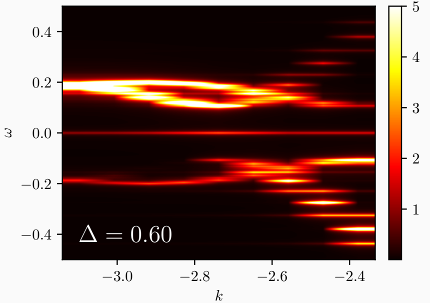

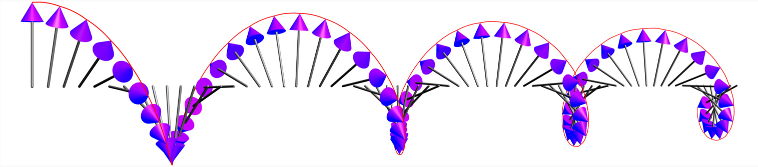

HELICAL SELFORGANISATION (TOPOFILIA)

A. Gorczyca-Goraj, T. Domański & M.M. Maśka, Phys. Rev. B 99, 235430 (2019).

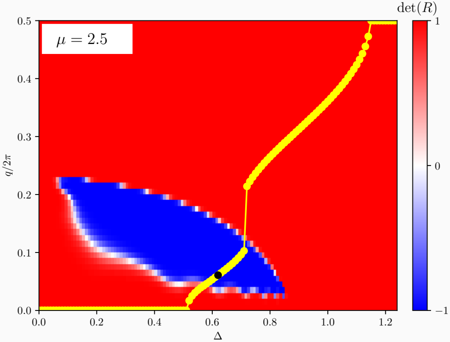

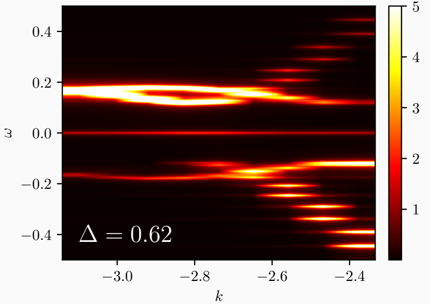

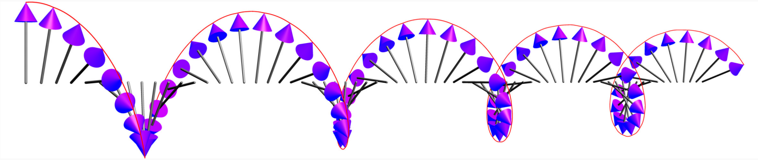

HELICAL SELFORGANISATION (TOPOFILIA)

A. Gorczyca-Goraj, T. Domański & M.M. Maśka, Phys. Rev. B 99, 235430 (2019).

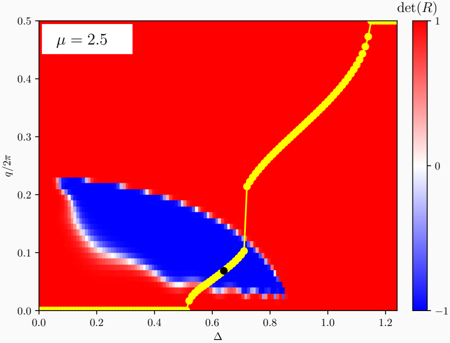

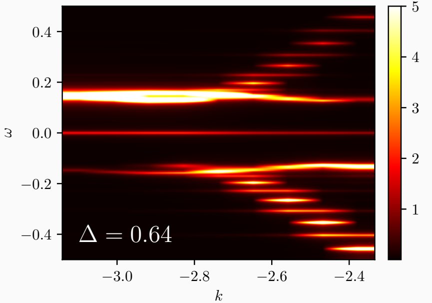

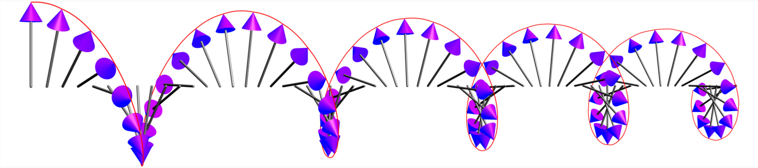

HELICAL SELFORGANISATION (TOPOFILIA)

A. Gorczyca-Goraj, T. Domański & M.M. Maśka, Phys. Rev. B 99, 235430 (2019).

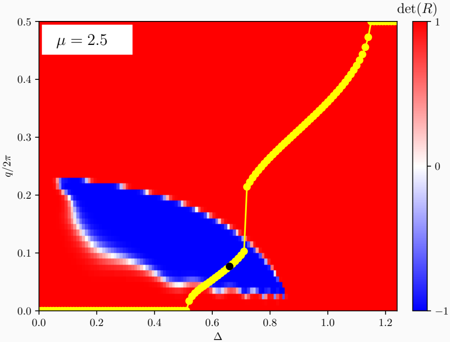

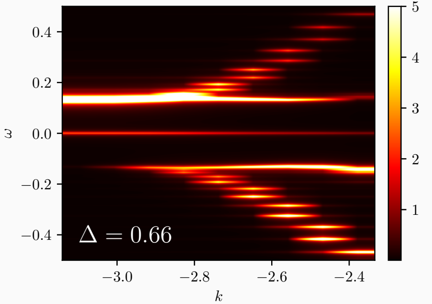

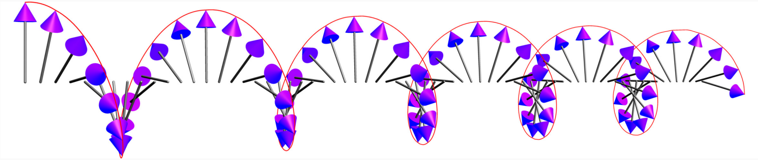

HELICAL SELFORGANISATION (TOPOFILIA)

A. Gorczyca-Goraj, T. Domański & M.M. Maśka, Phys. Rev. B 99, 235430 (2019).

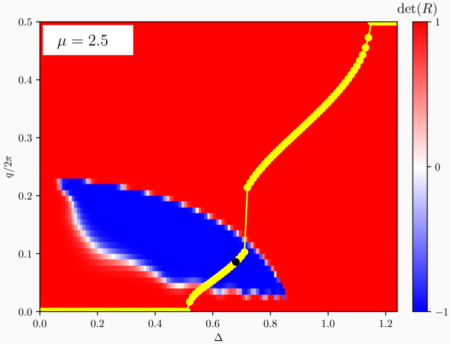

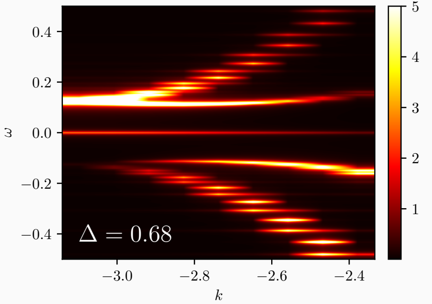

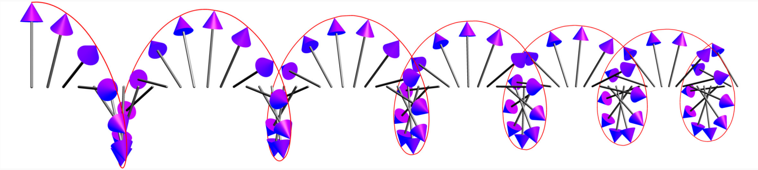

HELICAL SELFORGANISATION (TOPOFILIA)

A. Gorczyca-Goraj, T. Domański & M.M. Maśka, Phys. Rev. B 99, 235430 (2019).

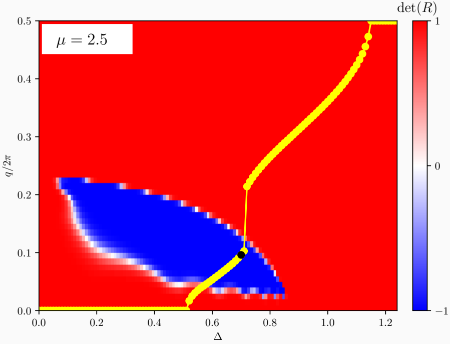

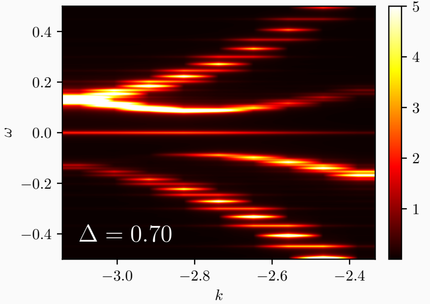

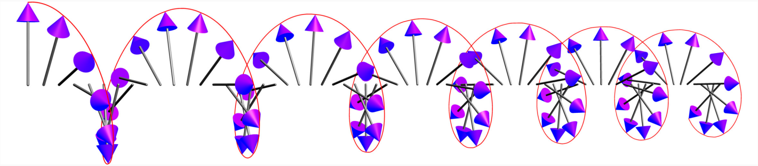

HELICAL SELFORGANISATION (TOPOFILIA)

A. Gorczyca-Goraj, T. Domański & M.M. Maśka, Phys. Rev. B 99, 235430 (2019).

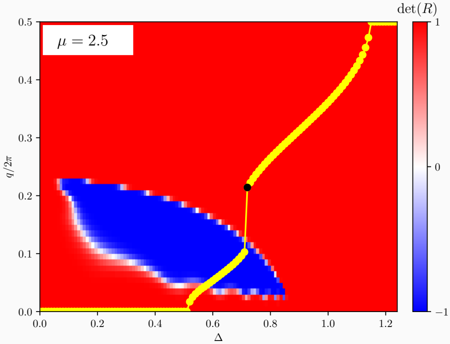

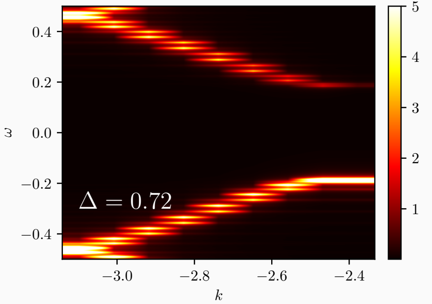

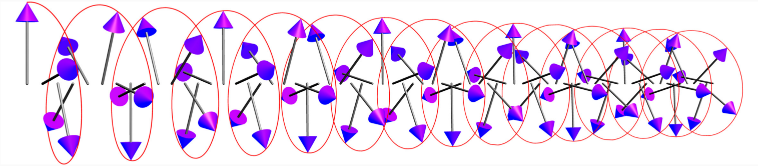

SPIRAL ORDER AT FINITE TEMPERATURES

Structure factor: $A(q) = \frac{1}{L}\sum_{jk} e^{iq(j-k)}\langle \vec{S}_j \cdot \vec{S}_k \rangle$

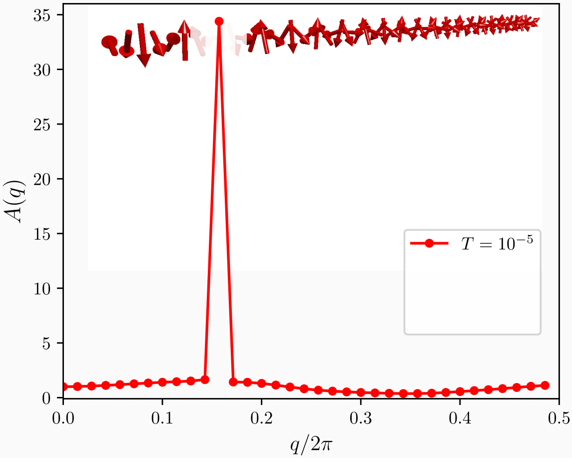

SPIRAL ORDER AT FINITE TEMPERATURES

Structure factor: $A(q) = \frac{1}{L} \sum_{jk} e^{iq(j-k)} \langle \vec{S}_j \cdot \vec{S}_k \rangle$

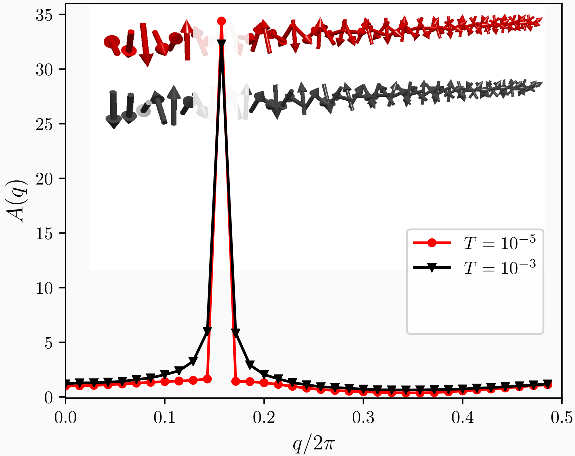

SPIRAL ORDER AT FINITE TEMPERATURES

Structure factor: $A(q) = \frac{1}{L} \sum_{jk} e^{iq(j-k)} \langle \vec{S}_j \cdot \vec{S}_k \rangle$

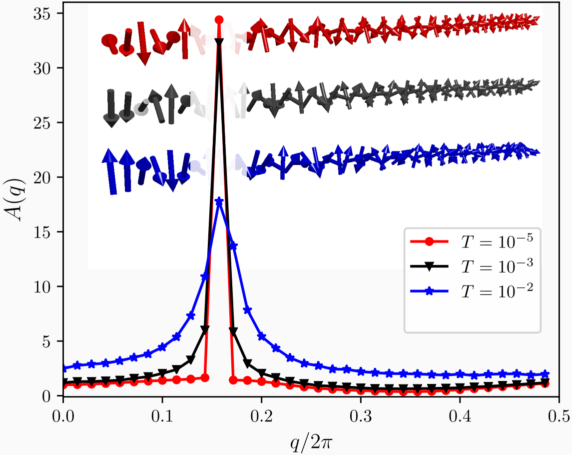

SPIRAL ORDER AT FINITE TEMPERATURES

Structure factor: $A(q) = \frac{1}{L} \sum_{jk} e^{iq(j-k)} \langle \vec{S}_j \cdot \vec{S}_k \rangle$

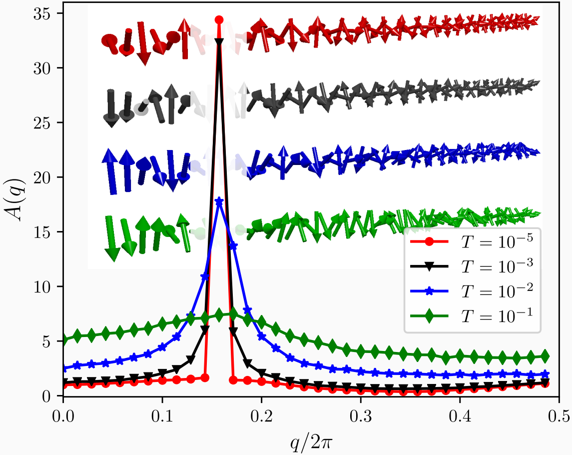

TEMPERATURE EFFECT ON MAJORANA QPS

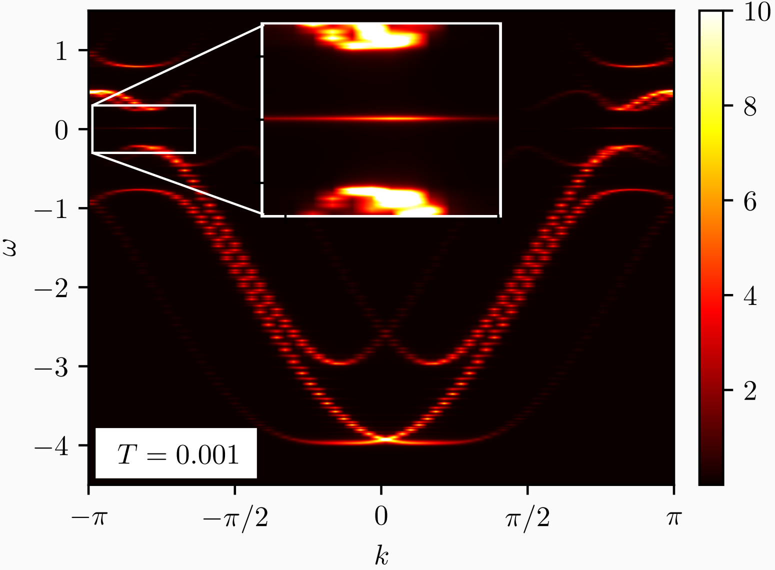

INFLUENCE OF TEMPERATURE ON MAJORANA QPS

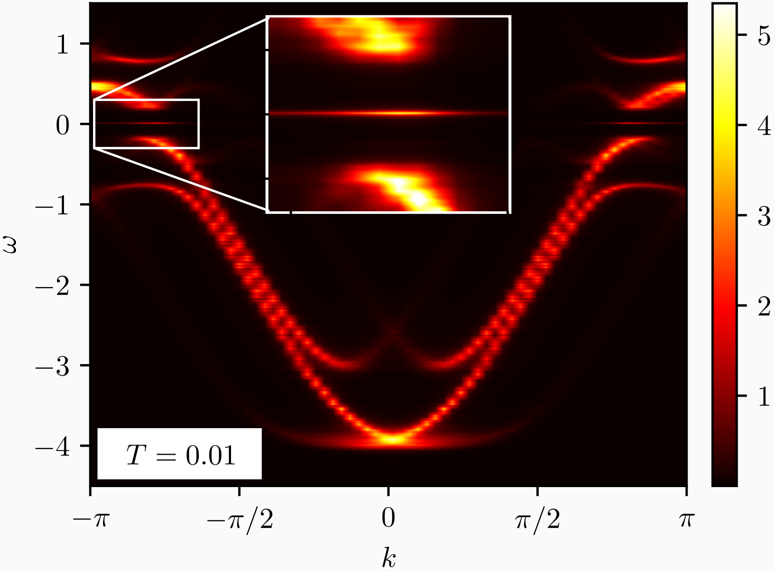

INFLUENCE OF TEMPERATURE ON MAJORANA QPS

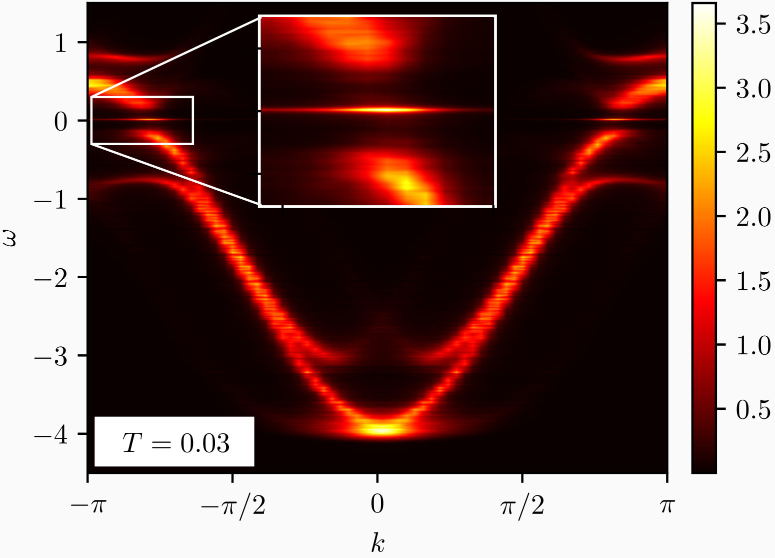

INFLUENCE OF TEMPERATURE ON MAJORANA QPS

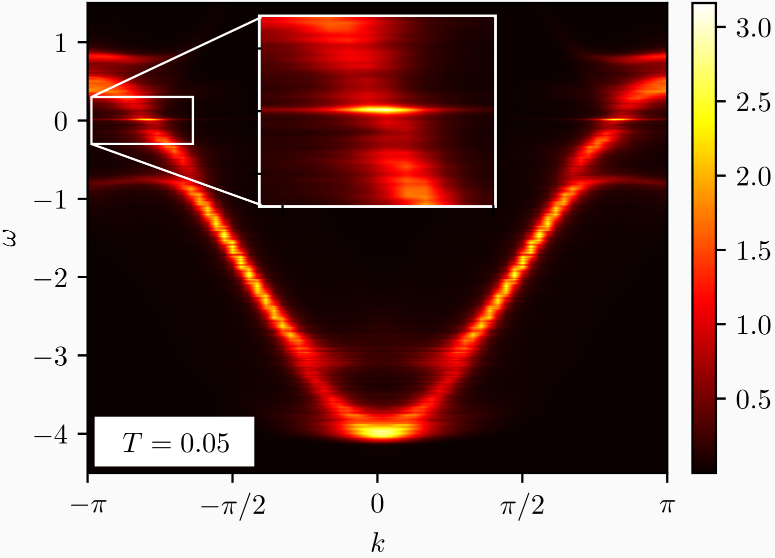

INFLUENCE OF TEMPERATURE ON MAJORANA QPS

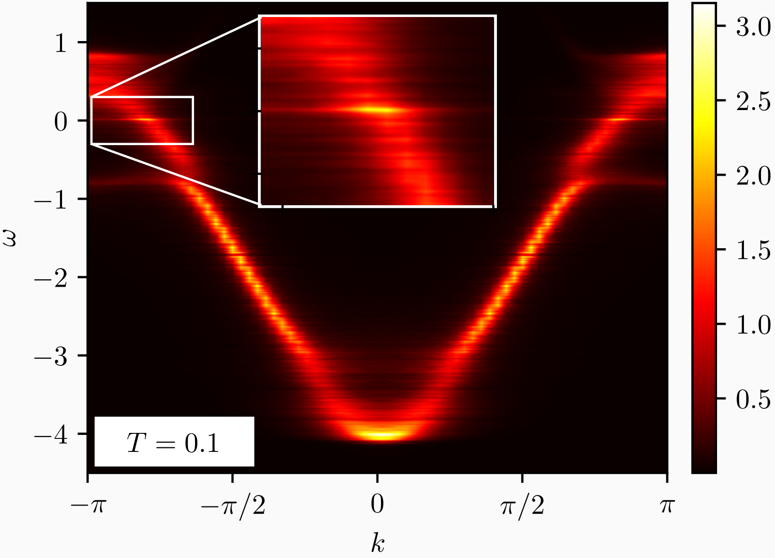

INFLUENCE OF TEMPERATURE ON MAJORANA QPS

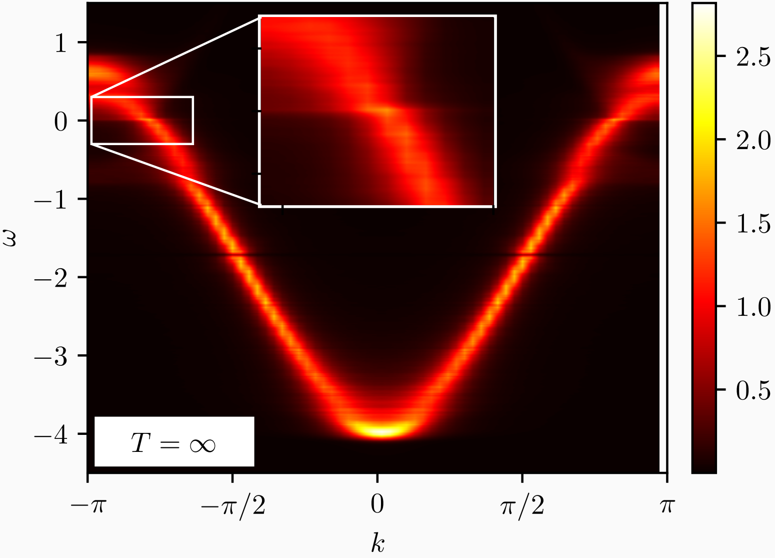

3. Magnetic ladders

TOPOLOGICAL MAGNETIC LADDER

Spiral magnetic order in a ladder deposited on conventinal superconductor.

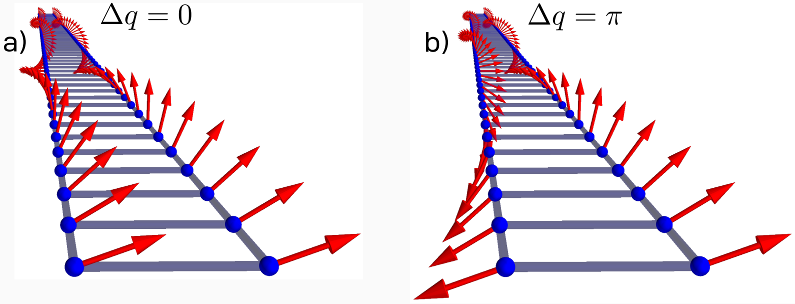

M.M. Maśka, N. Sedlmayr, A. Kobiałka, T. Domański, Phys. Rev. B 103, 235419 (2021).

TOPOLOGICAL PHASES

In thermodynamic limit ($N \to \infty$) we have determined the topological invariant $\mathbb{Z}$ of this system, which belongs to class AIII.

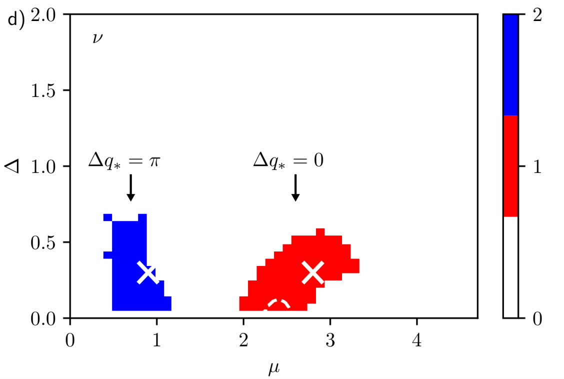

Regions of the topological superconducting phase are characterized by either antiparallel or parallel spiral arrangements of the magnetic ladder.

UNCONVENTIONAL TOPOLOGICAL TRANSITIONS

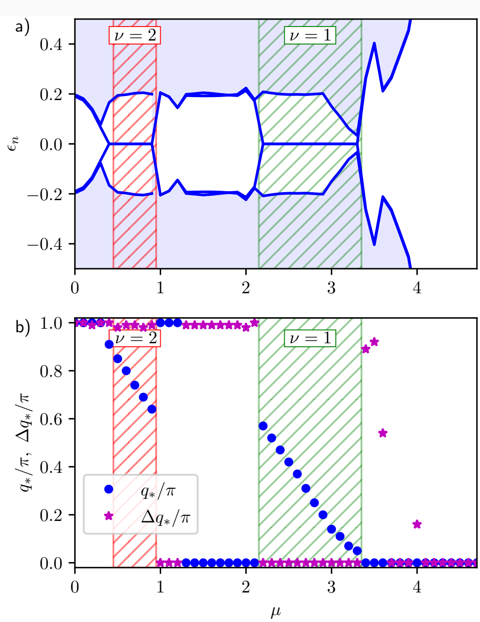

Variation of eigenenergies ε_n against μ for $\Delta = 0.3$

Variation of $q_\star$ and $\Delta q_\star$

UNCONVENTIONAL TOPOLOGICAL TRANSITIONS

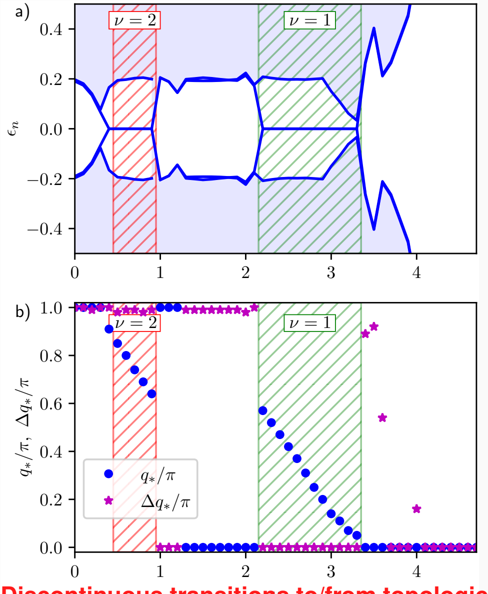

Variation of eigenenergies ε_n against μ for $\Delta = 0.3$

Variation of $q_\star$ and $\Delta q_\star$

Discontinuous transitions to/from topological phase without gap closing!

DISCONTINUOUS TRANSITIONS

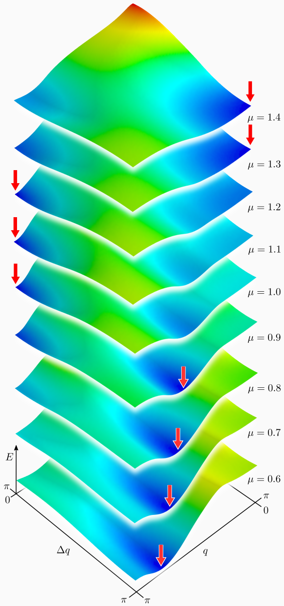

Total energy as function of q and Δq obtained for $\Delta = 0.3t$ and several μ.

Red arrows indicate the minimum energy.

BEYOND COPLANAR CONFIGURATIONS

a) $\mu = 0.2$

b) $\mu = 0.6$

c) $\mu = 1.6$

d) $\mu = 3.2$

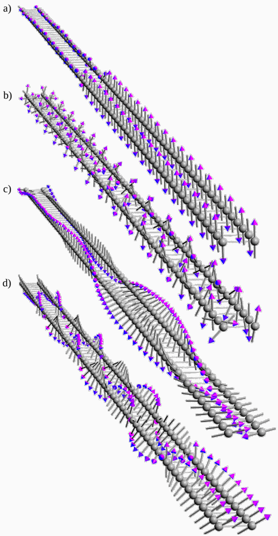

Unconstrained spin configurations obtained by the simulated annealing algorithm, performing the Metropolis Monte Carlo calculations (at low temperatures).

Majorana modes in Josephson junctions

PLANAR JOSEPHSON JUNCTIONS

Two-dimensional electron gas of InAs epitaxially covered by a thin Al layer

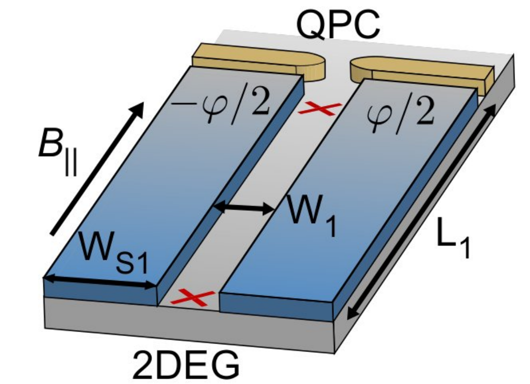

Width:

W_1 **= 80 nm**

Length:

L_1 **= 1.6** μ**m**

A. Fornieri, ..., Ch. Marcus and F. Nichele, Nature 569, 89 (2019).

Niels Bohr Institute (Copenhagen, Denmark)

Two-dimensional HgTe quantum well coupled to 15 nm thick Al film

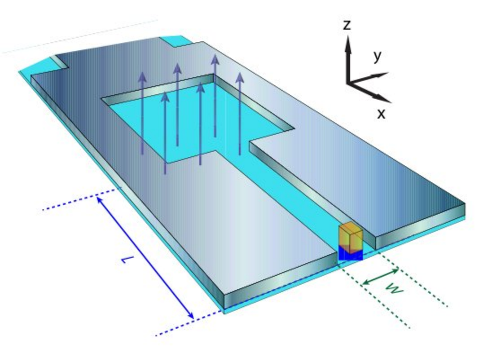

Width:

W = **600 nm**

Length:

L = **1.0 μm**

H. Ren, ..., L.W. Molenkamp, B.I. Halperin & A. Yacoby, Nature 569, 93 (2019).

Würzburg Univ. (Germany) + Harvard Univ. (USA)

PLANAR JOSEPHSON JUNCTIONS

Diagram of the trivial and topological superconducting state with respect to (1) phase difference ϕ and (2) in-plane magnetic field

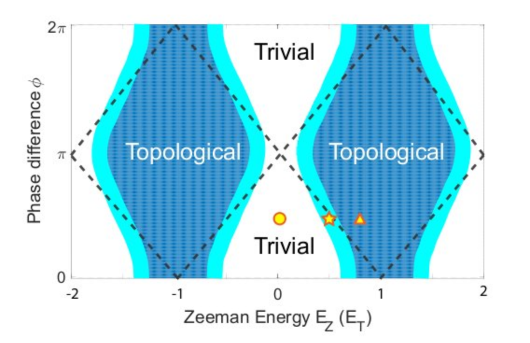

H. Ren, ..., L.W. Molenkamp, B.I. Halperin & A. Yacoby, Nature 569, 93 (2019).

Würzburg Univ. (Germany) + Harvard Univ. (USA)

TOPOGRAPHY OF MAJORANA MODES

Spatial profile of the zero-energy ($E_n = 0$) Majorana quasiparticles in a homogeneous metallic strip embedded into Josephson junction.

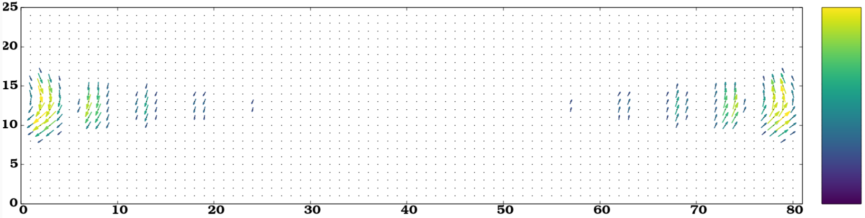

Sz. Głodzik, N. Sedlmayr & T. Domański, PRB 102, 085411 (2020).

LOCAL DEFECT IN JOSEPHSON JUNCTION

Spatial profile of the Majorana modes in presence of the strong electrostatic defect placed in the center.

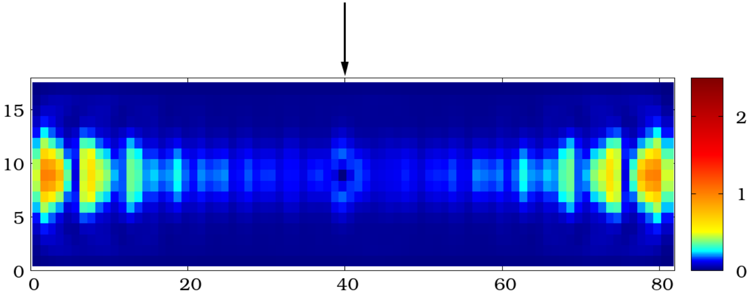

Sz. Głodzik, N. Sedlmayr & T. Domański, PRB 102, 085411 (2020).

LOCAL DEFECT IN JOSEPHSON JUNCTION

Spatial profile of the Majorana modes in presence of the strong electrostatic defect placed near the edge.

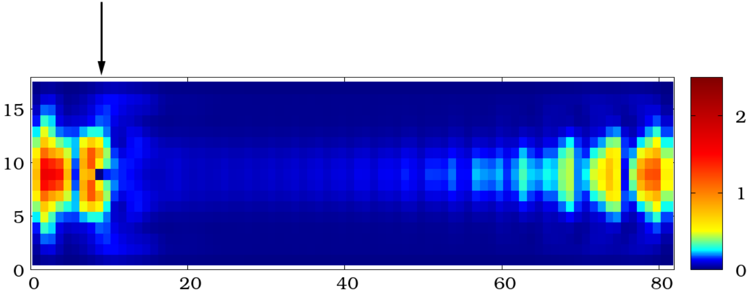

Sz. Głodzik, N. Sedlmayr & T. Domański, PRB 102, 085411 (2020).

LOCAL DEFECT IN JOSEPHSON JUNCTION

Spatial profile of the Majorana modes in presence of the strong electrostatic defect placed near the edge.

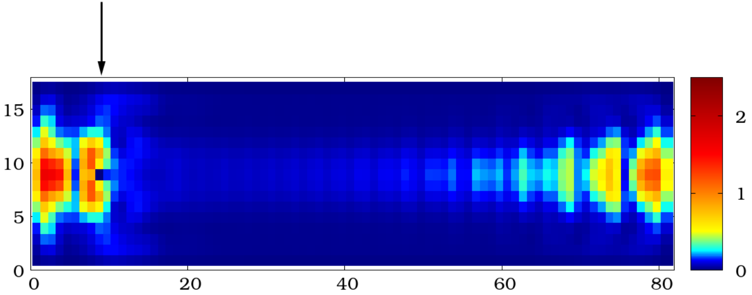

Sz. Głodzik, N. Sedlmayr & T. Domański, PRB 102, 085411 (2020).

"Benefits of Weak Disorder in One-Dimensional Topological Superconductors"

A. Haim & A. Stern, Phys. Rev. Lett. 122, 126801 (2019).

Higher-dimensional topological textures

Higher-dimensional topological textures

Platform for the chiral Majorana modes

TWO-DIMENSIONAL MAGNETIC STRUCTURES

Magnetic island of Co atoms deposited on the superconducting Pb surface

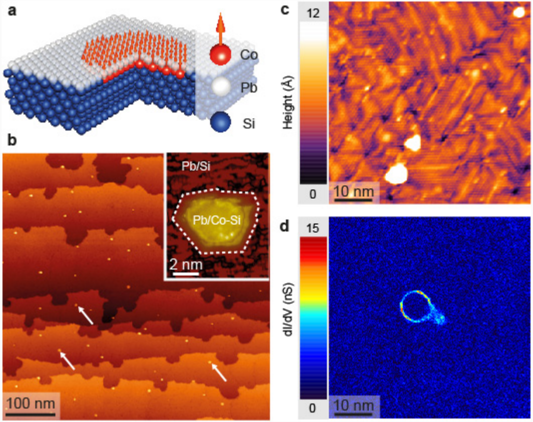

Diameter of island:

5 – 10 nm

G. Ménard, ..., and P. Simon, Nature Commun. 8, 2040 (2017).

Pierre & Marie Curie University (Paris, France)

PROPAGATING MAJORANA EDGE MODES

Magnetic island of Fe atoms deposited on the superconducting Re surface

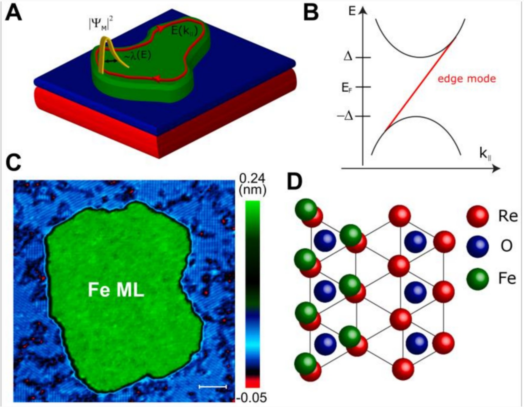

Chern number

C = 20

A. Palacio-Morales, ... & R. Wiesendanger, Science Adv. 5, eaav6600 (2019).

University of Hamburg (Germany)

VAN DER WAALS HETEROSTRUCTURES

Ferromagnetic island $CrBr_3$ deposited on superconducting $NbSe_2$

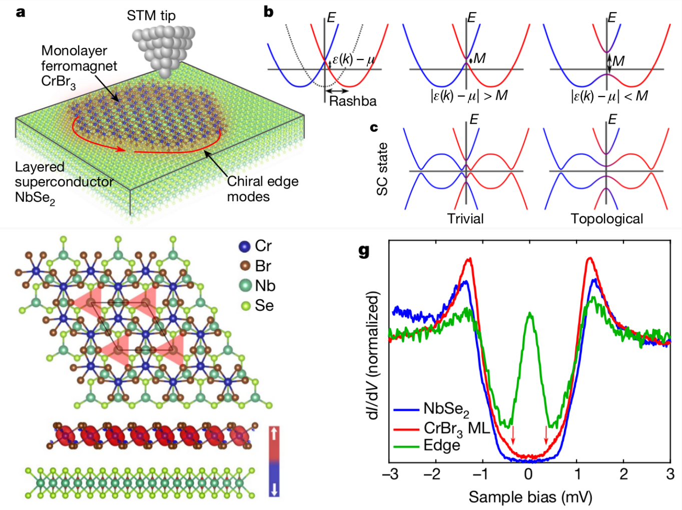

S. Kezilebieke ... Sz. Głodzik ... P. Lilienroth, Nature 424, 588 (2020).

MAGNETIC SKYRMION-TYPE TEXTURES

Scenario for topological superconductivity induced in 2D magnetic thin film hosting a skyrmion deposited on conventional s-wave superconductor

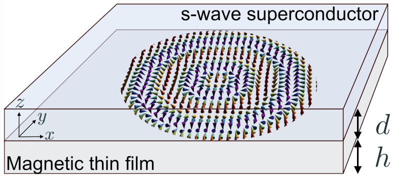

MAGNETIC SKYRMION-TYPE TEXTURES

Scenario for topological superconductivity induced in 2D magnetic thin film hosting a skyrmion deposited on conventional s-wave superconductor

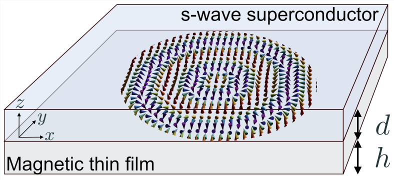

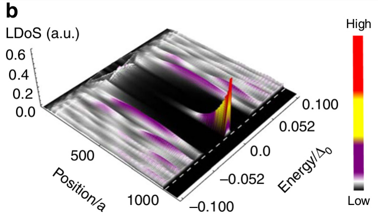

M. Garnier, A. Mesaros, P. Simon, Comm. Phys. 2, 126 (2019).

CONCLUSIONS

Synergy of magnetism and superconductivity in nanoscopic systems:

CONCLUSIONS

Synergy of magnetism and superconductivity in nanoscopic systems:

$\Rightarrow$ **allows for their constructive cooperation**

CONCLUSIONS

Synergy of magnetism and superconductivity in nanoscopic systems:

$\Longrightarrow$ **allows for their constructive cooperation**

$\Longrightarrow$ **inducing the topological states of matter**

CONCLUSIONS

Synergy of magnetism and superconductivity in nanoscopic systems:

$\Longrightarrow$ **allows for their constructive cooperation**

$\Longrightarrow$ **inducing the topological states of matter**

The resulting topological superconductors host the Majorana boundary modes which are promising for stable qubits & quantum computing.

COAUTHORS

⇒ **Maciek Maśka**

(Technical University, Wrocław)

⇒ **Nick Sedlmayr**

(M. Curie-Skłodowska University, Lublin)

⇒ **Aksel Kobiałka**

(M. Curie-Skłodowska University, Lublin)

Superconducting nanostructures: examples

normal metal (N) - quantum dot (QD) - superconductor (S)

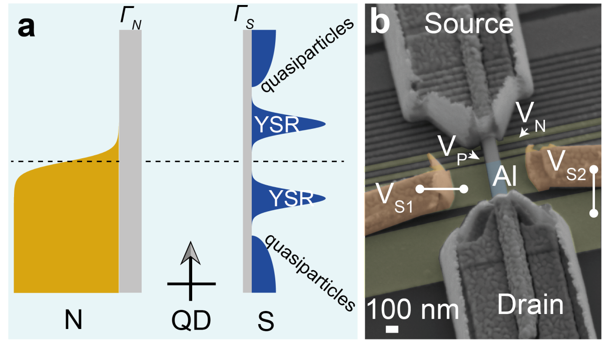

J. Estrada Saldaña, A. Vekris, V. Sosnovtseva, T. Kanne, P. Krogstrup, K. Grove-Rasmussen and J. Nygård, Commun. Phys. **3**, 125 (2020).

superconductor (S) - quantum dot (QD) - superconductor (S)

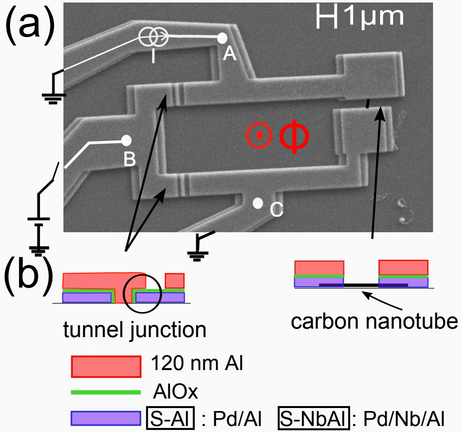

R. Delagrange, R. Weil, A. Kasumov, M. Ferrier, H. Bouchiat, R. Deblock, Phys. Rev. B **93**, 195437 (2016).

Dynamics of nanosuperconductors

QUENCH DRIVEN DYNAMICS

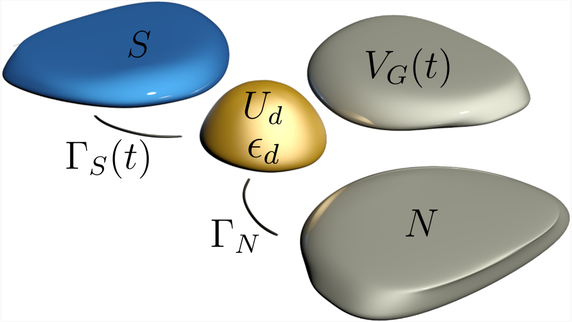

Possible quench protocols:

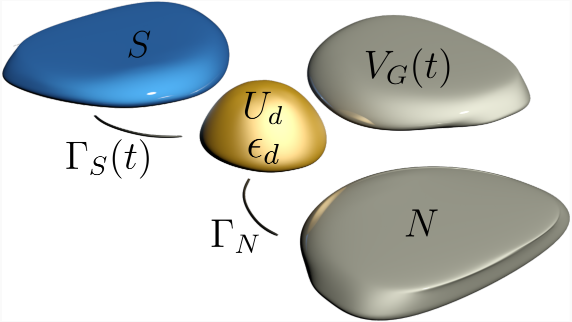

Possible quench protocols:

$\Rightarrow$ **sudden coupling to superconductor** $0 \to \Gamma_S$

QUENCH DRIVEN DYNAMICS

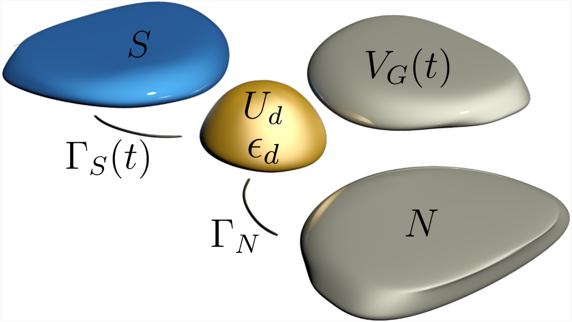

Possible quench protocols:

$\Longrightarrow$ **sudden coupling to superconductor** $0 \to \Gamma_S$

$\Longrightarrow$ **abrupt application of gate potential** $0 \to V_G$

K. Wrześniewski, B. Baran, R. Taranko, T. Domański & I. Weymann, PRB 103, 155420 (2021).

BUILDUP OF IN-GAP STATES

Schematics of the Andreev states formation induced by quench $0 \to \Gamma_S$

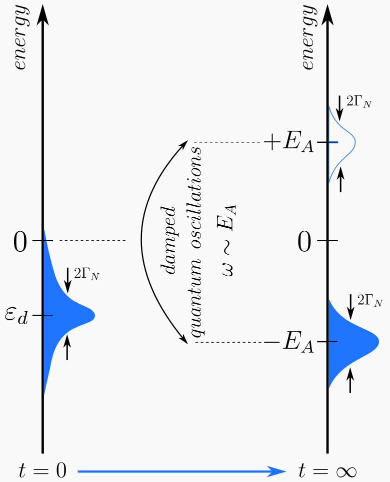

K. Wrześniewski, B. Baran, R. Taranko, T. Domański & I. Weymann, PRB 103, 155420 (2021).

BUILDUP OF IN-GAP STATES

Time-dependent observables driven by the quantum quench $0 \to \Gamma_S$

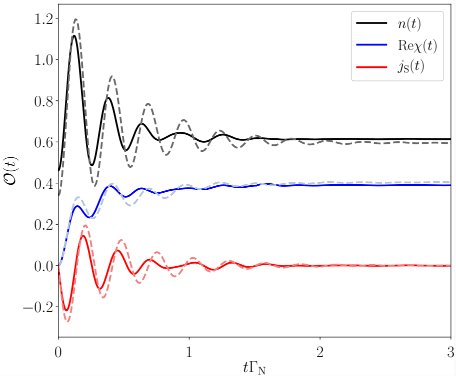

solid lines - time dependent NRG

dashed lines - Hartree-Fock-Bogolubov

K. Wrześniewski, B. Baran, R. Taranko, T. Domański & I. Weymann, PRB 103, 155420 (2021).

Singlet-doublet transition

SINGLY OCCUPIED VS BCS-TYPE CONFIGURATIONS

The proximitized quantum dot can described by

$$\hat{H}_{QD} = \sum_{\sigma} \epsilon_d \, \hat{d}^\dagger_\sigma \, \hat{d}_\sigma \; + \; U_d \, \hat{n}_{d\uparrow} \hat{n}_{d\downarrow} - \left(\Delta_d \, \hat{d}^\dagger_\uparrow \hat{d}^\dagger_\downarrow + \text{h.c.} \right)$$

SINGLY OCCUPIED VS BCS-TYPE CONFIGURATIONS

The proximitized quantum dot can described by

$$\hat{H}_{QD} = \sum_{\sigma} \epsilon_d \, \hat{d}^\dagger_\sigma \, \hat{d}_\sigma \, + \, U_d \, \hat{n}_{d\uparrow} \hat{n}_{d\downarrow} - \left(\Delta_d \, \hat{d}^\dagger_\uparrow \hat{d}^\dagger_\downarrow + \text{h.c.} \right)$$

Eigen-states of this problem are represented by:

$|\uparrow\rangle$ **and** $|\downarrow\rangle$ $\Leftarrow$ **doublet states (spin $\frac{1}{2}$)**

$$\left. \begin{array}{l} u\,|0\rangle - v\,|\uparrow\downarrow\rangle \\ v\,|0\rangle + u\,|\uparrow\downarrow\rangle \end{array} \right\} \Leftarrow$$ **singlet states (spin 0)**

SINGLY OCCUPIED VS BCS-TYPE CONFIGURATIONS

The proximitized quantum dot can described by

$$\hat{H}_{QD} = \sum_{\sigma} \epsilon_d \, \hat{d}^{\dagger}_{\sigma} \, \hat{d}_{\sigma} \; + \; U_d \, \hat{n}_{d\uparrow} \hat{n}_{d\downarrow} - \Big(\Delta_d \, \hat{d}^{\dagger}_{\uparrow} \hat{d}^{\dagger}_{\downarrow} + \text{h.c.} \Big)$$

Eigen-states of this problem are represented by:

$|\uparrow\rangle$ **and** $|\downarrow\rangle$ $\Leftarrow$ **doublet states (spin $\frac{1}{2}$)**

$$\left. \begin{array}{l} u\,|0\rangle - v\,|\uparrow\downarrow\rangle \\ v\,|0\rangle + u\,|\uparrow\downarrow\rangle \end{array} \right\} \Leftarrow$$ **singlet states (spin 0)**

Upon varrying the parameters ε_d, U_d or Γ_S there can be induced quantum phase transition between these doublet/singlet states.

Dynamical quantum phase transition

QUENCH DYNAMICS

Initially, for $t < 0$:

$$\hat{H}_0 |\Psi_0\rangle = E_0 |\Psi_0\rangle$$

QUENCH DYNAMICS

Initially, for $t < 0$:

$$\hat{H}_0 \left|\Psi_0\right\rangle = E_0 \left|\Psi_0\right\rangle$$

At time $t = 0$:

$$\hat{H}_0 \longrightarrow \hat{H}$$

QUENCH DYNAMICS

Initially, for $t < 0$:

$$\hat{H}_0 |\Psi_0\rangle = E_0 |\Psi_0\rangle$$

At time $t = 0$:

$$\hat{H}_0 \longrightarrow \hat{H}$$

Schödinger equation $i\frac{d}{dt} |\Psi(t)\rangle = \hat{H} |\Psi(t)\rangle$ implies

$$|\Psi(t)\rangle = e^{-it\hat{H}} |\Psi_0\rangle$$

QUENCH DYNAMICS

Initially, for $t < 0$:

$$\hat{H}_0 |\Psi_0\rangle = E_0 |\Psi_0\rangle$$

At time $t = 0$:

$$\hat{H}_0 \longrightarrow \hat{H}$$

Schödinger equation $i\frac{d}{dt}|\Psi(t)\rangle = \hat{H}|\Psi(t)\rangle$ implies

$$|\Psi(t)\rangle = e^{-it\hat{H}} |\Psi_0\rangle$$

Fidelity (similarity) of these states at time $t \geq 0$

$$\langle \Psi(t)|\Psi_0\rangle = \left\langle \Psi_0 | e^{-it\hat{H}} | \Psi_0 \right\rangle$$

Initially, for $t < 0$:

$$\hat{H}_0 \left|\Psi_0\right\rangle = E_0 \left|\Psi_0\right\rangle$$

At time $t = 0$:

$$\hat{H}_0 \longrightarrow \hat{H}$$

Schödinger equation $i\frac{d}{dt}\left|\Psi(t)\right\rangle = \hat{H}\left|\Psi(t)\right\rangle$ implies

$$\left|\Psi(t)\right\rangle = e^{-it\hat{H}}\left|\Psi_0\right\rangle$$

Fidelity (similarity) of these states at time $t \geq 0$

$$\left\langle\Psi(t)|\Psi_0\right\rangle = \left\langle\Psi_0|e^{-it\hat{H}}|\Psi_0\right\rangle$$

Loschmidt amplitude

STATIONARY VS DYNAMICAL PHASE TRANSITION

Idea: M. Heyl, A. Polkovnikov, S. Kehrein, Phys. Rev. Lett. 110, 135704 (2013).

STATIONARY VS DYNAMICAL PHASE TRANSITION

Idea: **M. Heyl, A. Polkovnikov, S. Kehrein, Phys. Rev. Lett. 110, 135704 (2013).**

Partition function

$$\mathcal{Z} = \left\langle e^{-\beta \hat{H}} \right\rangle$$

Loschmidt amplitude

$$\left\langle \Psi_0 \middle| e^{-it\hat{H}} \middle| \Psi_0 \right\rangle$$

STATIONARY VS DYNAMICAL PHASE TRANSITION

Idea: M. Heyl, A. Polkovnikov, S. Kehrein, Phys. Rev. Lett. 110, 135704 (2013).

Partition function

$$\mathcal{Z} = \left\langle e^{-\beta\hat{H}} \right\rangle$$

where

$$\beta = \frac{1}{k_B T} \longleftrightarrow it$$

Loschmidt amplitude

$$\left\langle \Psi_0 | e^{-it\hat{H}} | \Psi_0 \right\rangle$$

Loschmidt echo $L(t)$

$$L(t) = \left| \left\langle \Psi_0 | e^{-it\hat{H}} | \Psi_0 \right\rangle \right|^2$$

STATIONARY VS DYNAMICAL PHASE TRANSITION

Idea: M. Heyl, A. Polkovnikov, S. Kehrein, Phys. Rev. Lett. 110, 135704 (2013).

Partition function

$$\mathcal{Z} = \left\langle e^{-\beta \hat{H}} \right\rangle$$

where

$$\beta = \frac{1}{k_B T} \longleftrightarrow it$$

Free energy $F(T)$

$$\mathcal{Z} \equiv e^{-\beta F(T)}$$

Loschmidt amplitude

$$\left\langle \Psi_0 \middle| e^{-it\hat{H}} \middle| \Psi_0 \right\rangle$$

Loschmidt echo $L(t)$

$$L(t) = \left| \left\langle \Psi_0 \middle| e^{-it\hat{H}} \middle| \Psi_0 \right\rangle \right|^2$$

Return rate $\lambda(t)$

$$L(t) \equiv e^{-N\lambda(t)}$$

STATIONARY VS DYNAMICAL PHASE TRANSITION

Idea: **M. Heyl, A. Polkovnikov, S. Kehrein, Phys. Rev. Lett. 110, 135704 (2013).**

Partition function

$$\mathcal{Z} = \left\langle e^{-\beta \hat{H}} \right\rangle$$

where

$$\beta = \frac{1}{k_B T} \longleftrightarrow it$$

Free energy $F(T)$

$$\mathcal{Z} \equiv e^{-\beta F(T)}$$

Critical temperature T_c

nonanalytical $\lim_{T \to T_c} F(T)$

Loschmidt amplitude

$$\left\langle \Psi_0 | e^{-it\hat{H}} | \Psi_0 \right\rangle$$

Loschmidt echo $L(t)$

$$L(t) = \left| \left\langle \Psi_0 | e^{-it\hat{H}} | \Psi_0 \right\rangle \right|^2$$

Return rate $\lambda(t)$

$$L(t) \equiv e^{-N\lambda(t)}$$

Critical time t_c

nonanalytical $\lim_{t \to t_c} \lambda(t)$

SSH: QUENCH FROM NONTOPO → TOPO-PHASE

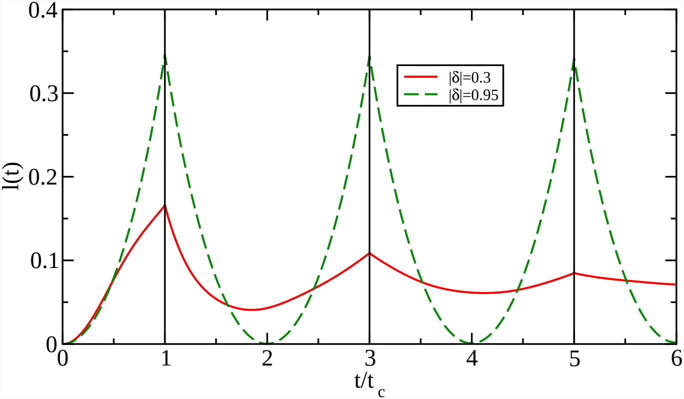

$$\hat{H} = -J\sum_{j}\left[\left(1+\delta e^{i\pi j}\right)\hat{c}_j^\dagger\ \hat{c}_{j+1}\ +\ \text{h.c.}\right]$$

solid red line $|\delta| = 0.3$

dashed green line $|\delta| = 0.95$

ISING MODEL: QUENCH OF g

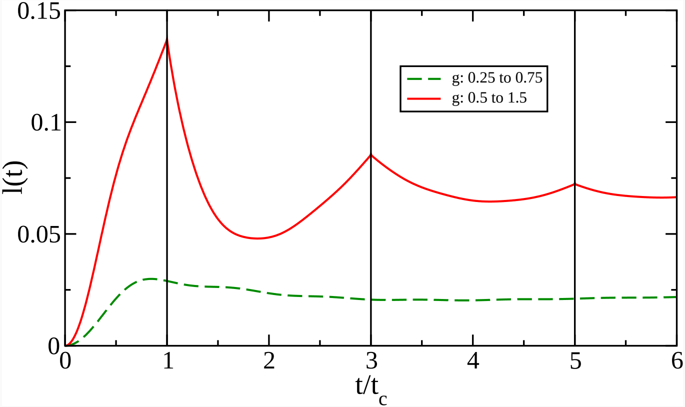

$$\hat{H} = -\frac{1}{2}\sum_{j=1}^{N-1} \hat{\sigma}_j^z \, \hat{\sigma}_{j+1}^z + \frac{g}{2}\sum_{j=1}^{N} \hat{\sigma}_j^x$$

solid red line - **across a phase transition**

dashed green line - **inside a phase transition**

WHAT ABOUT FINITE-SIZE SYSTEMS ?

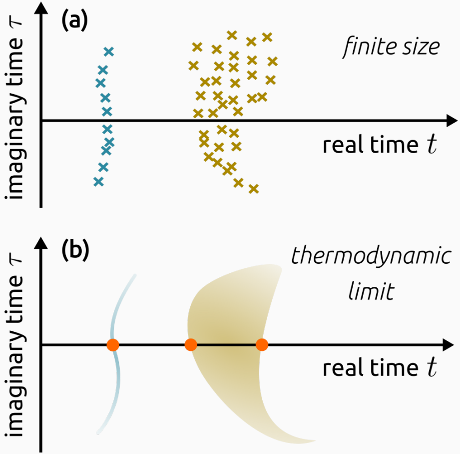

Schematic view of "Fisher zeros" obtained for the Loschmidt amplitude $\left\langle \Psi_0 | e^{-iz\hat{H}} | \Psi_0 \right\rangle$ in the complex plane $z = t + i\tau$.

Marcus Heyl, Rep. Prog. Phys. 81, 054001 (2018).

ISING MODEL: DQPT OF FINITE-SIZE SYSTEM

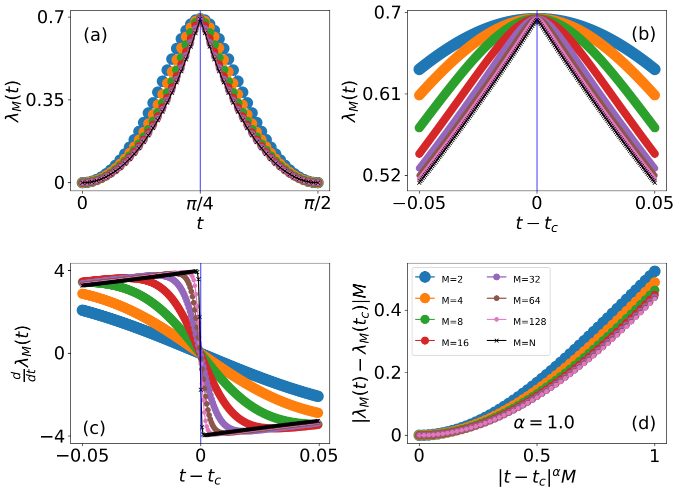

"Local measures of dynamical quantum phase transitions"

J.C. Halimeh, D. Trapin, M. Damme & M. Heyl, Phys. Rev. B 104, 075130 (2021).

Singlet-doublet DQPT

tNRG RESULTS: ABRUPT CHANGE OF Γ_S

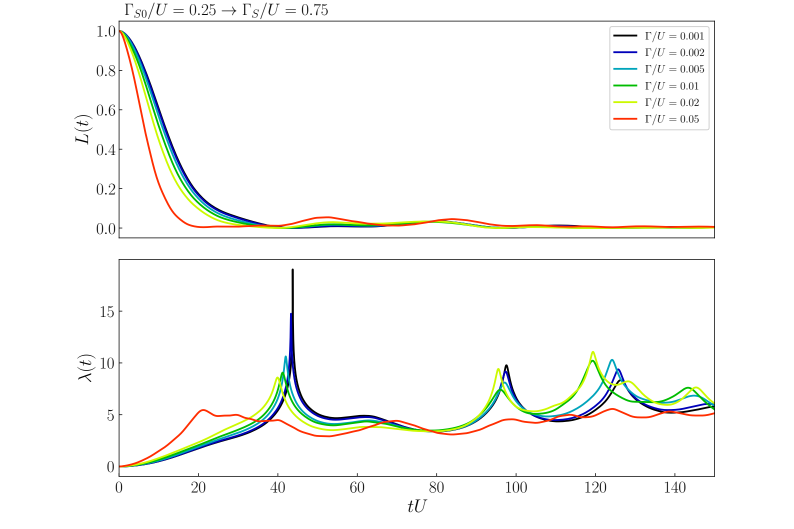

Loschmidt ampl. $L(t)$ and return rate $\lambda(t)$ obtained for various $\Gamma_N \equiv \Gamma$

*t*NRG RESULTS: ABRUPT CHANGE OF Γ_S

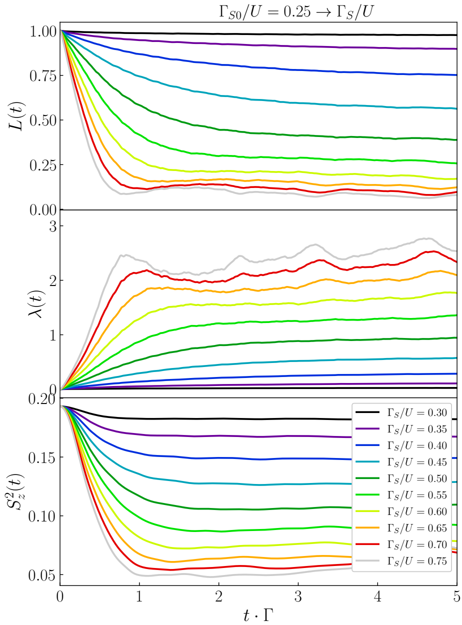

Loschmidt echo

$$L(t) \equiv |\langle \Psi(t) | \Psi(0) \rangle|^2$$

Return rate

$$|L(t)| \equiv e^{-N\lambda(t)}$$

The squared magnetic moment $\langle S_z^2(t) \rangle$

CONCLUSIONS

Quench imposed on N-QD-S (or S_L-QD-S_R) nanostructure:

- **rescales/develops in-gap quasiparticles**

CONCLUSIONS

Quench imposed on N-QD-S (or S_L-QD-S_R) nanostructure:

- **rescales/develops in-gap quasiparticles**
- **activating Rabi-type oscillations** **(due to particle-hole mixing)**

CONCLUSIONS

Quench imposed on N-QD-S (or S_L-QD-S_R) nanostructure:

- **rescales/develops in-gap quasiparticles**
- **activating Rabi-type oscillations** **(due to particle-hole mixing)**
- **and can exhibit dynamical QPT** **(upon varying ground states)**

CONCLUSIONS

Quench imposed on N-QD-S (or S_L-QD-S_R) nanostructure:

- rescales/develops in-gap quasiparticles
- activating Rabi-type oscillations (due to particle-hole mixing)
- and can exhibit dynamical QPT (upon varying ground states)

These phenomena would be detectable in transport properties.

ACKNOWLEDGEMENTS

- dynamical singlet-doublet phase transition

$\Longrightarrow$ K. Wrześniewski (Poznań), I. Weymann (Poznań),

N. Sedlmayr (Lublin),

- dynamics of in-gap states (transients effects, etc.)

$\Longrightarrow$ R. Taranko (Lublin), B. Baran (Lublin),

- time-dependent leakage of Majorana qps

$\Longrightarrow$ J. Barański (Dęblin)